NASA TECHNICAL NOTE

NASA TN D-4173

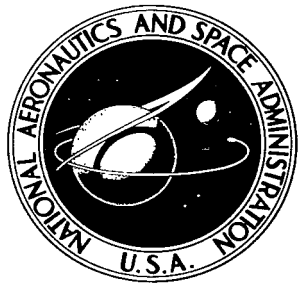

NASA TN D-4173

ANALYSIS OF STRESS-RUPTURE AND CREEP PROPERTIES OF TUNGSTEN-FIBER-REINFORCED COPPER COMPOSITES

by David L. McDanels, Robert A. Signorelli, and John W. Weeton

Lewis Research Center
Cleveland, Ohio

NATIONAL AERONAUTICS AND SPACE ADMINISTRATION • WASHINGTON, D. C. • SEPTEMBER 1967

NASA TN D-4173

ANALYSIS OF STRESS-RUPTURE AND CREEP PROPERTIES OF TUNGSTEN-FIBER-REINFORCED COPPER COMPOSITES

By David L. McDanels, Robert A. Signorelli, and John W. Weeton

Lewis Research Center
Cleveland, Ohio

NATIONAL AERONAUTICS AND SPACE ADMINISTRATION

For sale by the Clearinghouse for Federal Scientific and Technical Information
Springfield, Virginia 22151 – CFSTI price $3.00

CONTENTS

ANALYSIS OF STRESS-RUPTURE AND CREEP PROPERTIES OF TUNGSTEN-FIBER-REINFORCED COPPER COMPOSITES

by David L. McDanels, Robert A. Signorelli, and John W. Weeton

Lewis Research Center

SUMMARY

An analysis of the creep-deformation behavior of fiber-reinforced metallic composites was developed. Equations for predicting the creep rate and stress-rupture properties of fiber-reinforced metallic composites were presented. Stress-rupture and creep tests were conducted at 1200° and 1500° F on tungsten-fiber-reinforced copper composites. The results of these tests were used to verify the validity of the equations developed in the analysis. A discussion was presented relating the results obtained with the model system to more practical fiber-reinforced composite systems for stress-rupture applications. The stress-rupture strengths obtained with the tungsten-copper model system compared favorably with those of existing superalloys and demonstrated the potential of fiber-reinforced metallic composites in stress-rupture applications at elevated temperatures.

INTRODUCTION

Considerable effort is being directed toward the creation of composite materials to meet the demands of advancing technology for improved structural materials. One such material under investigation is the fiber-reinforced metallic composite in which a metallic matrix is reinforced with high-strength fibers.

The room-temperature tensile properties of fiber-reinforced metallic composites are very promising. Tungsten-fiber-reinforced copper was chosen as a model system in the composite work conducted at the Lewis Research Center because both components were insoluble in each other, and thus the properties of the composite could be compared directly with the properties of the components. The results of these studies, first reported in 1959 (refs. 1 and 2), established that the room-temperature ultimate tensile strength of the composites obeyed the concept of combined action and exhibited a law-of-mixtures type relation with fiber content. Further work at the Lewis Research Center on the stress-

strain behavior of tungsten-fiber-reinforced copper composites (refs. 3 and 4) showed that the stress at any value of strain could be predicted with the same law-of-mixtures relation, with appropriate stress values taken from the stress-strain curves of the component materials. The modulus of elasticity and yield strength (refs. 3 and 4), as well as the electrical conductivity (ref. 5), also obeyed this relation. Verification of this type of behavior for tungsten-copper and other metal-matrix composites was reported in references 6 to 8. Research at the Lewis Research Center (refs. 9 and 10) later extended these results to show that the elevated-temperature tensile properties of tungsten-fiber-reinforced copper and copper-alloy composites could also be predicted, using the same equations valid at room temperature, up to the maximum temperature tested, 1800° F.

The results of these investigations showed that the room-temperature and elevated-temperature tensile strength of materials can be increased considerably through reinforcement with high-strength fibers. In fact, tungsten-fiber-reinforced copper composites were made at NASA with room-temperature tensile strengths of over a quarter of a million pounds per square inch. Although there are applications for composite materials with a high tensile strength, there are also many applications for materials with a high stress-carrying capacity for long times at elevated temperatures. Applications such as advanced turbojet engines and space power generators are of immediate interest, and these applications require materials with higher stress-rupture strength and stress-rupture-strength-density properties than are available with current conventional materials. Such advanced applications have stimulated much interest in the use of fiber-reinforced composites to meet these materials requirements.

Some exploratory studies conducted to investigate the stress-rupture properties of fiber-reinforced composites showed increases in the rupture properties of various matrices by the reinforcement of titanium with molybdenum fibers (ref. 11), superalloys with tungsten fibers (refs. 12 and 13), and aluminum with boron filaments. In most of these studies, however, no attempts were made to relate the properties of the composites to those of the components. The fiber contents of the composites reported in these references were also relatively low. In addition, most of these composites had components that were soluble in each other, and, as shown in references 14 and 15, solubility may have a great effect on the properties of fiber-reinforced composites.

Recent work reported in reference 16 showed that 5-mil-diameter tungsten wire had stress-rupture properties that were superior to those of bulk tungsten and many other candidate materials for use in the temperature range of 1200° to 2500° F for rupture times beyond 200 hours. The stress-rupture results obtained for tungsten wire, the encouraging stress-rupture results reported in references 11 to 13 as well as the results and analyses reported earlier in references 1 to 8, indicate that fiber-reinforced metallic composites have a promising potential for use as structural materials for long-time, high-temperature applications. In view of these encouraging results, fiber-reinforced com-

posites appear to be promising materials, and an investigation of the stress-rupture behavior of a model system would be valuable in providing some insight into the strengthening mechanisms and deformation behavior of fiber-reinforced metallic composites.

The objectives of this investigation were as follows: to study the stress-rupture and creep rate properties of a model system, tungsten-fiber-reinforced copper composites; to relate these properties to those of the components; to develop an analysis of the behavior of composites that will allow the prediction of the properties of composites of this type; to gain an insight into the creep behavior and failure mechanisms of fiber-reinforced-composites under stress-rupture conditions; and finally, to determine from the data of the model system whether the projected stress-rupture properties of more practical fiber-reinforced composites would be high enough for use at elevated temperatures.

Stress-rupture tests were conducted on continuous-length fiber composites, and rupture times and creep rates were determined over a range of stresses and fiber contents at temperatures of 1200° and 1500° F. The stress-rupture properties of tungsten wires, annealed at composite fabrication conditions, were determined over this temperature range, while the stress-rupture and creep rate properties of copper were determined, also.

MATERIALS, APPARATUS, AND PROCEDURE

Materials

Previous work done on fiber-reinforced composites at the Lewis Research Center (refs. 1 to 5, 9, 10, 14, and 15) was conducted using a model system of tungsten-fiber-reinforced copper. The choice of this system permitted comparison with the previous studies.

Tungsten wire. - Commercially obtained, drawn-tungsten-filament wire (General Electric type 218CS) was selected as the reinforcement for the composites in this investigation because of its high stress-rupture strength and high recrystallization temperature. A fiber diameter of 5 mils was chosen because this diameter represented a good compromise between optimum properties and relative ease of handling.

Copper. - High-purity OFHC copper was selected as the matrix material to produce a model composite system. Copper was chosen because of its insolubility with tungsten, its melting point, and its ability, when molten, to wet tungsten.

Specimen Preparation

Figure 1 shows the steps involved in fabrication and specimen preparation. The composites were prepared by liquid-phase infiltration. To ensure axial orientation, continuous lengths of tungsten wire were placed in ceramic tubes and infiltrated with molten copper. Chemically cleaned copper rods were placed in the ceramic tube above the fiber bundle, and the whole assembly was heated. The specimen rods were infiltrated at 2200° F; 1/2 hour in hydrogen and 1/2 hour in a vacuum. After infiltration, the specimen rods were removed from the ceramic tubes and centerless ground into specimens. A drawing of the specimen used is shown in figure 2. Typical specimen cross sections are shown in figure 3.

Stress-Rupture Testing

Single fibers. - Individual specimen wires were stress rupture tested. These wires were annealed using the same time, temperature, and atmospheric conditions that were used for composite infiltration. The inside of the filament stress-rupture testing chamber is shown in figure 4. This apparatus was specifically designed for stress-rupture testing of small-diameter fibers.

For this test, the wire was strung through a tantalum-wound resistance furnace and around a pulley and attached to a weight pan. The top of the chamber was then replaced and the system evacuated to a measured vacuum of about 5×10^{-5} to 1×10^{-6} torr. The furnaces were then turned on and allowed to stabilize at the desired test temperature. The temperatures were monitored with a platinum - platinum-13-percent-rhodium thermocouple placed at the midpoint of the furnace about 1 millimeter away from the test wire. During the test, the temperature did not vary more than $\pm2^{\circ}$ F. After stabilization, the weights were applied to the specimen wires. The friction in the pulley was determined to be less than 0.5 percent. When the wire specimen failed, the weight pan turned off a microswitch which stopped an elapsed time meter. Additional details on the experimental procedure used for testing fibers may be found in references 16 and 17.

Copper. - Copper rods were annealed in a vacuum for 4 hours at 1500° F. The rods were given this treatment to crystallize fully the material and to ensure a large grain size comparable to that encountered in the composites. The rods were then machined by centerless-grinding into test specimens. A larger diameter, 0.200 inch, was used in the test section of the copper specimens because of the low stresses encountered. The specimens were then placed in conventional stress-rupture machines and tested at temperatures of 1200° and 1500° F in a purified helium atmosphere. The load on the specimens was applied by either a 10:1 or 20:1 lever arm. The temperature was measured by three

Chromel-Alumel thermocouples attached to the test section. The temperature was held at the desired test temperature with a $\pm 2^{\circ}$ F variation. When the specimen failed, the lever arm attached to the weight pan hit a microswitch and turned off an elapsed time meter.

Composites. - Composite test specimens were tested in conventional creep machines as described previously. The weight was applied by a 20:1 lever arm. Again the temperature was monitored by three Chromel-Alumel thermocouples and controlled to within $\pm 2^{\circ}$ F of the desired test temperature. Tests were run at temperatures of 1200° and 1500° F. Creep measurements were taken for both the copper and the composites by dial gage readings.

Composite Measurements

The initial diameters of the composites were measured with a micrometer, and the loads for the desired stresses on the composites were calculated from these diameters.

The fiber contents of the composites were determined after failure by sectioning the failed specimen transversely in an area immediately adjacent to the fracture, but outside the necked region. These sections were then mounted, polished, and photographed. The wires were counted, and the fiber content was calculated from this wire count and from the original area.

RESULTS

Stress-Rupture Results

Tungsten wire. - The results of stress-rupture tests conducted on 5-mil-diameter tungsten fibers are presented in table I and are plotted in figure 5. The data points represent the results of tests conducted on wire that had received an annealing treatment duplicating the infiltration treatment. The properties of the fibers were determined in the condition in which they existed in the composite. The dashed line shown in this figure represents a least-squares fit of the results of stress-rupture tests conducted on as-received tungsten wire of the same diameter as that reported in reference 16. The solid line represents a least-squares fit of the data for annealed wire from the present investigation. Table II shows the stress for several rupture lives, taken from these calculations at 1200° and 1500° F. These data show that the stress-rupture life of the tungsten wire was improved slightly by the annealing treatment, which indicates that annealing tungsten wire is not nearly as detrimental to the stress-rupture properties at elevated temperature

as it was to the room-temperature tensile properties. References 3 and 4, for example, showed that the room-temperature tensile strength of tungsten wire was reduced about 25 percent by a similar annealing treatment.

Copper. - The results of stress-rupture tests on annealed copper-copper specimens are presented in table III and are plotted in figure 6. Tests were conducted at temperatures of 1200° and 1500°. As indicated in figures 5 and 6, the stresses to cause rupture for copper are very small in relation to those for the tungsten wire. A least-squares fit of these data is presented in table IV, which shows the stress for several rupture times of copper at each temperature.

Composites. - Stress-rupture tests on tungsten-fiber-reinforced copper composites were conducted at various stresses at test temperatures of 1200° and 1500° F. Fiber contents ranged from 4 to 75 volume percent with rupture times to about 1100 hours. The data are tabulated in tables V and VI and are plotted in figures 7 and 8 on the basis of a log fiber content - log rupture time for composite stresses tested at 1200° and 1500° F respectively. There is a linear relation between these variables, although there is some scatter in the data. A least-squares fit of the data was calculated for each stress and is shown by the lines in figures 7 and 8.

Creep Rate Results

Tungsten wire. - The filament stress-rupture testing apparatus was designed to obtain only stress-rupture data, and thus no direct measurement of the creep rate of the tungsten fibers used in this investigation could be made.

Copper. - A typical creep curve for copper specimens tested at 1200° F is shown in figure 9; the curves obtained at 1500° F were similar. The creep rates of several copper specimens tested at 1200° and 1500° are presented in table VII and are plotted in figure 10. Table VIII shows the results of least-squares fits of stress required to cause selected creep rates at each of these temperatures. A plot of the log rupture time - log creep rate for copper specimens tested at 1200° and 1500° F is shown in figure 11. The curves for these two temperatures almost coincide.

Composites. - A typical creep curve for composites tested at 1500° F is shown in figure 12. The curve shows that the composites undergo first- and second-stage creep, with some indication of third-stage creep. The second-stage creep appears to be linear, and thus a creep rate may be determined. It was impossible to measure the amount of initial creep of the specimens, since the dial gage indicator measured the elongation of all parts of the loading train. A typical creep curve for composites tested at 1200° F is shown in figure 13. The same general trends shown in figure 12 are present in this fig-

ure, also; however, there appears to be a greater amount of third-stage deformation before failure.

A plot of log rupture time - log creep rate for composites is shown in figure 14. Although there is considerable scatter in this data, there appears to be a linear relation between these two variables at both 1200° and 1500° F, and the curves for each temperature are parallel. These data also indicate that, for a given rupture time, the creep rate for composites tested at 1200° F will be lower than that for those tested at 1500° F.

The creep rates of various composite specimens tested at 1200° and 1500° F are presented in table IX. Several of the specimens were tested solely to determine creep rates; thus, the rupture times for these specimens are not listed. The results from this table are plotted on a log fiber content - log creep rate basis for each composite stress used (figs. 15 and 16). A series of parallel lines were obtained over the stress range tested.

DISCUSSION

Prediction of Creep Rate of Composites

In the subsequent analysis and calculations, the interrelations of the parameters controlling the stress-rupture and creep properties of fiber-reinforced composites, under conditions of constant-load tensile creep at elevated temperatures, are presented. This analysis is based on the following assumptions:

(1) Strains in the fiber and the matrix are equal to each other and are equal to those of the composite.

(2) The fiber area A_f plus the matrix area A_m are equal to the area of the composite A_c, which is taken as unity.

(3) Composites are reinforced with longitudinally oriented fibers and are tested in the direction parallel to the reinforcement.

(4) Components of the composites are insoluble.

(5) Tensile failure of both the fiber and the matrix occurs.

From the results of references 3 and 4, the most significant parameters for the determination of the tensile properties of composites were the fiber content and the specific property under consideration of the fiber and the matrix. Therefore, it was expected that the same parameters would be equally important in the prediction of the stress-rupture and creep properties of composites.

If the equilibrium of forces is considered, the stress distribution on the components of the composite can be expressed by the equation

$$\sigma_c = \sigma_f A_f + \sigma_m A_m \quad \text{at a given creep rate } \dot{\epsilon}_i \tag{1}$$

where

σ	stress on each component
A	relative area of each component
$\dot{\epsilon}$	secondary creep rate
c	composite
f	fiber
m	matrix

This equation is similar in format to the equation (refs. 3 and 4) for predicting the stress on a composite at any value of strain.

Since, on the basis of the initial assumption the total creep elongation and creep rate of the composite, the fiber, and the matrix are equal, the stresses required to give the creep rate of the composite may be calculated from the properties of the components tested externally.

Creep curves of the individual components are determined at several stresses, as shown by the schematic curves of figure 17(a). The creep rate determined from the linear second-stage creep portion of these curves is then plotted as a function of stress on a log-log basis (fig. 17(b)). The linear relation thus obtained for the matrix can be expressed as

$$\log \sigma_m = \log\left(\sigma_m\right)_o + \psi_m \log(\dot{\epsilon}_m) \tag{2}$$

or

$$\sigma_m = \left(\sigma_m\right)_o (\dot{\epsilon}_m)^{\psi_m} \tag{3}$$

$$\sigma_f = (\sigma_f)_o (\dot{\epsilon}_f)^{\psi_f} \tag{4}$$

where σ is stress on one component tested individually, and subscript o denotes the stress required to give a creep rate of 1 percent per hour, ψ is slope of log stress - log creep rate curve.

The stress required on each component to cause a given creep rate of $\dot{\epsilon}_i$ could be determined from these data and substituted into equation (1).

Thus, at a given creep rate $\dot{\epsilon}_i$, equation (1) would have the form

$$\left(\sigma_c\right)_{\dot{\epsilon}_i} = \left(\sigma_f\right)_{\dot{\epsilon}_i} A_f + \left(\sigma_m\right)_{\dot{\epsilon}_i} A_m \qquad \text{at a constant creep rate } \dot{\epsilon}_i \tag{5}$$

where $\sigma_{\dot{\epsilon}_i}$ is the stress on each component, tested externally, which would cause a creep rate of $\dot{\epsilon}_i$.

Equation (5) may be used to predict the stresses required to cause a given creep rate of $\dot{\epsilon}_i$; however, to make these predictions more applicable to other creep rates, a more general substitution into equation (1) must be made. These stresses must be determined from data obtained on the individual components tested externally. The graphical process for the determination of these stresses is shown schematically in figure 17(c).

Substituting equations (3) and (4) into equation (1) results in

$$\sigma_c = \left(\sigma_f\right)_o \left(\dot{\epsilon}_f\right)^{\psi_f} A_f + \left(\sigma_m\right)_o \left(\dot{\epsilon}_m\right)^{\psi_m} A_m \tag{6}$$

which, since the creep rates are equal, becomes

$$\sigma_c = \left(\sigma_f\right)_o \left(\dot{\epsilon}^{\psi_f}\right)(A_f) + (\sigma_m)\left(\dot{\epsilon}^{\psi_m}\right)(A_m) \tag{7}$$

A graphical representation of equation (7) is shown schematically in figure 17(d). The effect of the exponents in this equation determines the stress selected for the end points of the schematic plot. A straight-line relation exists between the end point stresses thus selected, as in equation (5). For the situation where the exponents ψ_f and ψ_m are approximately equal or where the stress contribution of the fiber is much greater than that of the matrix, equation (7) may be simplified to the form

$$\sigma_c = \left[\left(\sigma_f\right)_o A_f + \left(\sigma_m\right)_o A_m\right]\dot{\epsilon}^{\psi} \tag{8}$$

or expressed as

$$\sigma_c = \left\{\left(\sigma_m\right)_o + A_f\left[\left(\sigma_f\right)_o - \left(\sigma_m\right)_o\right]\right\}\dot{\epsilon}^{\psi} \tag{9}$$

From this analysis, it is postulated that the creep rate of composites may be predicted by an exponential form of the law-of-mixtures equation.

Prediction of Stress-Rupture Life of Composites

Although the creep rate properties of fiber-reinforced composites may be directly related to the properties of the components, the relation of stress-rupture life to the properties of the components is not as direct or as straightforward. The stresses carried by the fiber and the matrix vary with time during the course of a creep test. The change in stress during primary creep generally is not too great and, therefore, is considered negligible in the present analysis. The stresses are considered constant during second-stage creep. However, with continuing time in the test, the weaker matrix component would tend to deviate from second-stage creep and to enter third-stage creep, except that it is prevented from doing so by the fibers. Stress changes on the components would result. Eventually both components may enter third-stage creep, which causes a further stress redistribution.

Prediction based on exact duplication of stresses on components. - To duplicate in external tests the conditions on the fiber and the matrix throughout the entire course of a stress-rupture test from initial loading to third-stage creep and failure, it would be necessary to test the component material with an infinite number of stresses or with a continuously varying load application on each component. If the exact loading were duplicated, the stress for a given rupture time of a composite could be determined exactly and would follow the relation

$$\sigma_c(t) = \sigma_f(t)A_f + \sigma_m(t)A_m = \text{constant} \tag{10}$$

where $\sigma_f(t)$ and $\sigma_m(t)$ vary with time in such a way that equation (10) is satisfied for all rupture times, and where these conditions can be duplicated in an external test. Since it would be most difficult to duplicate these conditions experimentally, it seems reasonable to make one of several possible approximations and simplifications to arrive at equations that can be handled easily to predict the rupture behavior of composites.

Prediction based on life-fraction of stresses on components. - The first simplification to develop equations that can predict the composite rupture behavior might be one in which the stress-rupture life could be considered a summation of the life-fraction spent in each state of a finite number of stages. For example, a case could be one in which the creep behavior of the composite were considered to be made up of primary, secondary, and tertiary creep, and one in which each component spent a certain portion of its life in each stage. The summation of these fractions could then be used to calculate the total life

of the composite. A method like this might be utilized, but it would represent relatively little simplification and is almost as difficult to perform experimentally as the previously discussed exact method.

Prediction based on stresses for rupture life of fiber and stresses for creep rate of matrix. - This method involves the assumptions that the fiber is the rate-controlling component and that the effect of the third-stage creep of the matrix can be ignored. The life of the composite may thus be considered largely dependent on the stronger, more brittle fiber, which would usually fail first, rather than dependent on the weaker, more ductile matrix. It is also assumed that the change in stress on the matrix, in going from second- to third-stage creep would be small relative to the stress carried by the fiber. This assumption implies that the rupture time of the fiber will not be changed significantly by the additional stress given up by the matrix, that the full life of the matrix will not be utilized, and, therefore, that the stresses on the fiber and the matrix are considered to be constant up to rupture.

The first step in using this prediction method would be to determine the creep curves of the components, as shown schematically in figure 18(a). For these data, it is necessary to obtain results that would give both the creep rate and the rupture-time data for each stress. The creep rate of the fiber, associated with a given rupture time, can be determined from a plot similar to that shown in figure 18(b). Thus, for a given rupture time, there is an associated creep rate of the fiber, the matrix, and the composite.

After the creep rate is established, the stress on the matrix which causes that creep rate may be determined from the log stress - log creep rate curve shown in figure 18(c). This stress on the fiber to cause rupture in a given time may be determined as shown in figure 18(d). The stresses on each component, due to the rupture time and the associated creep rate, are used as end points of the curve in figure 18(e). The behavior shown in this figure can be expressed by the equation

$$\left(\sigma_c\right)_t = \left[\left(\sigma_f\right)_t A_f\right] + \left[\left(\sigma_m\right)_{\dot{\epsilon}(t_f)} A_m\right] \tag{11}$$

where $\sigma_{m_{\dot{\epsilon}(t)}}$ is the stress on the matrix required to give the creep rate associated with a composite rupture time of t. To determine a more general expression of equation (11), shown schematically in figure 18(f), consider the following:

The fiber stress may be expressed by

$$\sigma_f = \left(\sigma_f\right)_1 t_f^{\omega_f} \tag{12}$$

where

$(\sigma_f)_1$ stress on fiber to cause rupture in 1 hour

t rupture time

ω slope of log stress - log rupture-time curve

The stress on the matrix at a given creep rate was expressed by equation (3). The log creep rate - log rupture-time plot, shown schematically in figure 18(b), for the composite may be expressed by

$$\dot{\epsilon}_f = \dot{\epsilon}_f\Big|_{t=1\,hr} t_f^{\gamma_f} \tag{13}$$

where $\dot{\epsilon}_f\Big|_{t=1\,hr}$ is the creep rate of the composite associated with a rupture time of 1 hour and γ_f is the slope of the log creep rate - log rupture-time curve of the fiber.

Since creep rates of the fiber, matrix, and composite are equal, then equation (13) may be substituted into equation (3) to give

$$(\sigma_m)_{\dot{\epsilon}(t_f)} = \sigma_m\Big|_{\dot{\epsilon}=1} \left(\dot{\epsilon}_c\Big|_{t=1} t_f^{\gamma_f}\right)^{\psi_m} \tag{14}$$

Substituting equations (12) and (14) into equation (11) gives the general form of this equation:

$$\sigma_c = \left[(\sigma_f)_1 t^{\omega_f} A_f\right] + \left[\sigma_m\Big|_{\dot{\epsilon}=1} \left(\dot{\epsilon}_f\Big|_{t=1} t_f^{\gamma_f}\right)^{\psi_m} A_m\right] \tag{15}$$

The rupture time of a composite could be predicted from equation (15) with a good accuracy when both the fiber and the matrix tested outside the composite have similar creep rates, or when the change in stress from the matrix to the fiber is small compared with the fiber stress calculated from the secondary creep rate, or when the shortening of fiber life resulting from the change in stress is small. This latter condition would be true for a large number of practical composites.

Unfortunately, the creep data required for the calculation of the matrix stress in equation (15) is not readily obtainable in the literature for many materials, since the use temperature for fiber-reinforced composites probably would be considerably higher than

the use temperature for the unreinforced material.

Prediction based on stresses for rupture time of components. - The final method to predict the stress-rupture life of composites is based on the more easily obtained handbook-type data. In this case, the stresses for a given rupture time of the fiber and the matrix can be related by

$$\left(\sigma_c\right)_t = \left[\left(\sigma_f\right)_t A_f + \left(\sigma_m\right)_t A_m\right]_{t=\text{constant}} \tag{16}$$

The analysis of this equation would be similar to that presented previously for the calculation of the creep rate. A linear relation exists between composite stress and fiber content, with the stress on each component, for a given rupture time, as the end points of the straight line. Equation (16) can be expanded to a more general form by considering the stress rupture properties of the fiber and the matrix tested externally. The fiber properties are given by equation (12), and the properties of the matrix can be represented by the same type of relation:

$$\sigma_m = \left(\sigma_m\right)_1 t^{\omega_m} \tag{17}$$

Substituting equations (12) and (17) into equation (16) gives

$$\sigma_c = \left[\left(\sigma_f\right)_1 t^{\omega_f} A_f\right] + \left[\left(\sigma_m\right)_1 t^{\omega_m} A_m\right] \tag{18}$$

If it is assumed that the fiber is the rupture-time-determining component, or if the slopes $\omega_f \cong \omega_m$, then equation (18) may be simplified to a more usable form:

$$\sigma_c = \left[\left(\sigma_f\right)_1 A_f + \left(\sigma_m\right)_1 A_m\right] t^{\omega_f} \tag{19}$$

or

$$\sigma_c = \left\{\left(\sigma_m\right)_1 + A_f\left[\left(\sigma_f\right)_1 - \left(\sigma_m\right)_1\right]\right\} t^{\omega_f} \tag{20}$$

Handbook-type values of the stress for a given rupture time for components may be used directly in equation (16) for prediction of the properties of composites. If the

stress-rupture properties of the components are known, these values may be used with equations (19) or (20) to determine the rupture time of composites.

Experimental Verification of Predictions

To verify the equations previously presented, the data obtained in this investigation on the behavior of tungsten-fiber-reinforced copper composites are analyzed. The first section deals with the prediction of the creep properties, and the second section deals with the prediction of stress-rupture properties.

Verification of creep rate predictions. - Creep rate data were obtained for unreinforced copper and for composites with several fiber contents tested at several stresses. The equipment used to test the tungsten fibers did not allow a determination of creep rate for the fibers. Thus, it will be attempted to verify these equations by calculating the stress required on the composite to cause a given creep rate at a given fiber content. The equations will also be used to calculate the stress required on the fiber to give a certain creep rate. The approach used for these verifications follows the format shown schematically in figure 17.

The minimum creep rate of unreinforced copper specimens at test temperatures of 1200° and 1500° F was determined from curves of the type shown in figure 9. The log stress - log creep rate plot (fig. 10) was then determined from these data. The linear behavior could be represented by equation (3).

The minimum creep rate of composites was determined from creep curves of composites (fig. (12) shows a typical example) at various stresses and fiber contents. These results were plotted on a log fiber content - log creep rate basis for each composite stress used. Typical examples of these plots are shown in figure 15. The fiber content intercept at various creep rates was calculated from the least-squares fit of these data and is plotted in figure 19 against composite stress for data from tests run at 1200° and 1500° F. The stress at the 100-volume-percent fiber intercept was calculated in the manner to be shown subsequently. The data for the fiber contents at each composite stress show a linear relation that is in agreement with equation (5). Although these plots show that the copper values are small and approach zero, an enlargement of the low-fiber-content region of this curve (fig. 20) shows that the linear relation is valid since good agreement is obtained for each creep rate for the matrix (fig. 10) and for the composites (fig. 15). Figure 20 shows that the lines for each creep rate pass through the stress values obtained from the externally tested unreinforced copper. These stress values, although low, are clearly separated and show that the matrix has a definite influence on the properties. The linear relation obtained in these curves shows that the equa-

tions presented are valid and that the end point plots verify the exponential functions of equations (7) to (9).

Because the creep-rate stress relation of the fiber could not be determined directly, it was necessary to calculate these values. Since the linear relation of the composite stress - fiber content was verified in the preceding section, equation (5) can be rewritten:

$$\left(\sigma_f\right)_{\dot{\epsilon}_i} = \left.\frac{\left(\sigma_c\right)_{\dot{\epsilon}_i}}{A_f} - \frac{\left(\sigma_m\right)_{\dot{\epsilon}_i}(1 - A_f)}{A_f}\right|_{\dot{\epsilon}_i = \text{constant}} \tag{21}$$

As indicated by this equation, the higher the stress the matrix can carry, the greater the matrix contribution and the lower the effective stress on the fiber for a given composite stress and fiber content. Equation (21) was used to calculate the composite fiber stresses, which were plotted with their experimentally determined composite creep rates in figure 21. This figure shows that there is good correlation between the log of the fiber stress and the log of the creep rate, which in turn serves as verification of equation (5). It is presumed that this method could be used to calculate the creep properties of fibers in composites where the creep properties are changed by a reaction between the fiber and the matrix within the composite. This method would be extremely valuable in situations where it would be impossible to duplicate the corresponding changes in the fiber external to the composite.

Verification of stress-rupture predictions. - The verifications of the stress-rupture property predictions are more difficult because of the approximations required; therefore, it was decided to verify equations (16) and (20) on the basis of the rupture time of each of the components. This method was more desirable than that using the matrix stresses in equations (11) and (15), based on creep rate. Since the matrix stresses in the creep rate plot of figure 10 were approximately the same as those shown in figure 6 for the rupture time, the method was considered justified.

The rupture times of unreinforced copper and of tungsten wire were determined experimentally as functions of stress (figs. 5 and 6) and were used in equations (13) and (17). The rupture time of composites was also determined and plotted as a function of fiber content (figs. 7 and 8) for each stress used. The intercepts from these plots were calculated for several rupture times and plotted in figure 22 for results from tests run at 1200° and 1500° F. These plots show that a law-of-mixtures type relation holds for stress-for-a-given-rupture-time with fiber content and serves as a verification of equation (16). The intercepts at the end points verify the exponential dependence expressed by equation (19).

Unfortunately the strength of the copper matrix used in this investigation was low, and it is not obvious from figure 22 that the matrix was carrying its full share of the load. The creep rate data presented earlier in figure 20, however, show that the copper was carrying its full share of the load in creep. It is expected that the copper matrix would also contribute its share to the stress-rupture life of the composite. Figure 22 shows that the fiber is contributing its full share to the composite stress. From the linearity of the data of figure 22 and its extrapolation to a value near zero, which approaches the matrix strength, it can be assumed that the matrix is contributing its share to the stress-rupture life of the composite.

These predictions were also verified by the calculation of the fiber stress from composite data:

$$\left(\sigma_f\right)_t = \left.\frac{\left(\sigma_c\right)_t}{A_f} - \frac{\left(\sigma_m\right)_t (1 - A_f)}{A_f}\right|_{t = \text{constant}} \tag{22}$$

The matrix stress selected was taken from the least-squares fit of the data obtained for unreinforced copper at the rupture time of the composite. The calculated fiber stresses are plotted in figure 23 as a function of the rupture time. This plot illustrates that the dashed line, representing a least-squares fit from the composite data, shows good agreement with the solid line, representing the data from the annealed tungsten wire. Again, this agreement indicates that the tungsten wire is contributing its full strength to the composite, and it can be assumed that the matrix is also doing the same.

Significance of verifications of analyses. - The equations presented and the subsequent verifications with experimental data indicate that the creep rate of composites should follow a law-of-mixtures behavior of composite stress for a given creep rate with fiber content. As long as both components are in second-stage creep and neither component has failed, this linear relation should hold. This behavior could be considered analogous to the behavior encountered for the condition when both components are elastic in a tensile test.

In the case of the prediction of rupture life for a composite, however, the situation is somewhat analogous to the tensile behavior when both components are in plastic flow. In this latter case, the full tensile strength of the fiber is being used in the composite, but the matrix stress used is that of the stress-strain curve at the value of strain where the fiber fails, not at the value of its ultimate tensile strength. As mentioned in the section Prediction of Stress-Rupture Life of Composites, the full life of the matrix may not be usable from the prediction of the stresses on the matrix in a composite. The stress carried by the matrix will approximate more closely the stress carried at the creep rate established for the composite by the fiber. Also there will be a critical fiber content

below which the matrix will be the rupture-time-controlling component. This critical fiber content will become appreciable with increasing matrix strength. In the situation where the matrix strength approaches the fiber strength for a given rupture time and where the matrix exhibits considerably more elongation at failure, calculations of rupture lives from equations (15) and (20) will be in increasing error. Although the fiber may be stronger, the matrix will be sufficiently strong to creep after the fibers have fractured. In the situation where the fiber content is below the critical content, the entire stress-rupture life of the matrix may be utilized, and rupture may not occur for a long time after the fracture of the fibers. This situation would give rise to a discontinuity in the stress-fiber content curve for rupture in a given time comparable to the discontinuity observed in references 3, 4, and 8 for tensile testing. Thus, for these conditions, it must be remembered that the predictions of stress-rupture life presented in this report are first approximations, and additional data will be required for the determination of the properties of composites having higher strength matrices.

Effect of Fiber Matrix Interactions on Prediction of Creep Rate and Stress-Rupture Life

The predictions based on the previously presented equations were made on the assumption that the composite was ideal, that is, that the properties of the components were the same within the composite as when tested externally. As shown by a review of the effects of interfacial reactions (ref. 18) as well as by the work reported in references 7, 9, 10, 14, and 15, nonideal situations may exist in actual composites in which the properties of the components, primarily the fiber, have sometimes been severely reduced by fiber-matrix interaction. For stress-rupture applications, the elevated temperature and long times involved might be expected to increase the degradation of properties resulting from interaction.

Although the equations developed in the preceding sections were based on a model composite system, the analysis may be extended to other nonideal composite systems. The strength of the fibers in nonideal systems varies with reactivity, which is dependent on the time and temperature encountered by the composite during fabrication and testing. In addition, it is usually impossible to determine the properties of reacted fibers outside the composites. Although reacted fibers may be removed from the composites by dissolution, there is always the possibility that the dissolution may affect their properties.

The equations presented for the prediction of the creep and stress-rupture properties of nonreactive model composites may be applicable, with a slight modification, to reactive composites. With a reactive system, it may be assumed that the properties of the

matrix are essentially unaffected by the fiber-matrix interaction. This assumption seems valid since the tensile properties of copper-alloy-matrix composites were unaffected by their reaction with tungsten fibers (refs. 9 and 10); therefore, the matrix properties may be determined in the same way as were those of the model composite. The stress-rupture time or stress-creep rate relation of the matrix can be determined by external testing. A limited amount of composite data would also be required and would consist of a few composite specimens in which the composite stresses and the fiber contents could be varied at random. With the stress-rupture life or creep rate results obtained, the fiber stress can be calculated using equations (22) or (21), respectively. These calculations would give the properties of the fiber, in the condition it exists within the composite, and would take into account any change in properties due to interaction with the matrix. Once the properties of the fiber have been determined, then the composite stress - fiber content curves similar to those shown in figures (22) or (20) can be drawn. From this data, extrapolations can be made to predict the properties of composites for a wide range of fiber contents and composite stresses.

The methods of predictions presented allow the extrapolation of a limited amount of composite data to a more general case for an entire composite system. In addition, the methods are useful in determining fiber properties within composites where the fiber properties cannot be determined externally, such as the cases for a reacted fiber or for directionally solidified composites.

Creep Behavior of Fiber-Reinforced Composites

The micromechanics of the tensile behavior of fiber-reinforced composites were presented in references 3, 4, and 8. In view of the insight gained into the creep behavior of tungsten-fiber-reinforced copper composites, the micromechanics of these composites in creep are now discussed. To aid in this discussion, a schematic plot of the creep-deformational behavior of a typical composite and its components is shown in figure 24. Note that the creep rate curves for the composite (fig. 24(c)) and the matrix and the fiber in the composite (dashed portion of fig. 24(d) and (e)) are identical.

During the initial loading of composites for a stress-rupture test, the test is analogous to a high-temperature tensile test where each component of the composite carries a portion of the load. The behavior of the components can be predicted by using the equations presented in reference 5. After a stress equilibrium is established by the condition imposed during the initial loading, the composite starts to elongate with time. During the course of this time-dependent, decreasing creep rate, there is a continuing rebalancing of stresses between the fiber and the matrix components of the composite. If the entry

into second-stage creep occurs at different times for the two components, then the stronger component, usually the fiber, forces the weaker component to adopt its behavior after a short transition period. This change in the normal behavior of the components gives rise to a quasi first-stage creep.

Eventually a balance is reached between work-hardening and recovery, and a constant creep rate is achieved. With the attainment of a constant creep rate, there is additional rebalancing and redistribution of stresses between the components. This stress equilibrium is maintained for a period of time. The effect of stress and fiber content on the creep rate was discussed previously.

After a period of second-stage creep, most materials pass into third-stage creep. Again, the passage into third-stage creep of the components of the composite may occur at different times. Materials such as copper (fig. 9) showed a considerable amount of third-stage creep. Similar results were observed for copper in reference 19. From the data obtained for composites in the present investigation, it appears that the tungsten wire remained in second-stage creep for a much longer time than did copper. This behavior tends to be true for many of the fibers under consideration for use as reinforcements in composites for stress-rupture applications. Since the fiber and the matrix are bonded together in the composite, the stronger, rate-controlling component, the fiber, forces the more ductile, more easily deformed component, the matrix, to remain in second-stage creep. This process gives rise to a quasi second-stage creep behavior in the composite. This behavior causes the stress on the matrix to be reduced to a value that will enable it to remain in second-stage creep. This lowering of the stress on the matrix is compensated by an increase in stress on the fiber. Quasi second-stage behavior would be expected to continue until the rate-controlling component entered third-stage creep at which time a new stress distribution would be set up. This process would continue until the initiation of fracture.

Fracture Behavior of Tungsten-Fiber-Reinforced Copper Composites

Eventually the balance attained in second-stage creep is disturbed, and the composite passes into some degree of third-stage creep. The deviation from second-stage creep in a composite may be attributed to two factors: the rate-controlling component may enter third-stage creep and/or the fibers may start to fail.

The schematic diagram of the stress-rupture failure triangle presented in figure 25 may serve as a model to illustrate the discussion of failure behavior. This figure shows a schematic plot of the log stress on the fiber in a composite against the log of the rupture time. The lines represent the scatter band of the fibers.

During third-stage creep, fibers fractured within the test section of a composite

specimen. The individual reinforcing fibers in a composite are considered to have a certain scatter of failure time at a given stress. The fibers within the composite would be expected to have a similar scatter band as those tested externally. The first fiber to break (pt A) would establish the minimum rupture time for the fibers in the composite. This time is represented by t_{min} in the schematic plot of figure 25. The maximum rupture time for the fibers in the composite would be shown in this figure as t_{max}, which is the point at the upper limit of the fiber scatter band lying on a horizontal line starting at point A', slightly above point A. Point A represents the stress on the fiber that failed at t_{min}. Since that fiber failed, the remaining cross section of the composite must support a stress slightly higher than that originally encountered when all the fibers were intact.

If all the remaining fibers exhibited no scatter and had perfectly uniform rupture times lying at the top line of the scatter band, then failure would not occur until t_{max}. If the rupture times lay at the lower line of the scatter band, then rupture would occur immediately at a rupture time of t_{min}. In most cases, however, the rupture times would be a random mixture of all values lying within the stress-rupture triangle. With each successive fiber fracture, the actual stress on the remaining fibers would increase and decrease the size of the triangle. Eventually, the stress will exceed the strength of the remaining fibers, and fracture of the composite will occur. The schematic in figure 25 shows that the failure of the first fiber does not necessarily cause immediate fracture of the composite. The actual fracture time would be determined by the number of fibers present and by the scatter band of the fibers themselves.

In room-temperature tensile tests, the stresses could be carried across the ends of the broken fibers by shear through the matrix. This stress transfer is dependent on a strong bond between the fiber and the matrix and on a sufficient shear strength of the bond and the matrix to carry these stresses. As the temperature increases, the bond strength decreases. As shown in reference 8, the shear strength of the matrix also decreases much more rapidly than the tensile strength, which causes an increase in the required length-diameter ratio to give efficient reinforcement. Thus, as a fiber breaks, a greater ineffective length (that length which does not efficiently carry a shear load) increases.

The usual interpretation of shear strength deals with the short-time properties. In a composite of this type, under stress-rupture conditions, the longtime properties are of prime interest. There are almost no data available for the longtime stress-rupture properties of materials in shear, but it is expected that they would be even lower than those of the short-time data. Therefore, the breaking of the fibers would probably cause a greater reduction in the effective reinforcement in stress rupture than had been shown for tensile properties.

The actual fractures encountered in this investigation of the stress-rupture properties of tungsten-fiber-reinforced copper composites is now discussed. Examples of each type

of fracture are discussed and illustrated with a macro- and a microphotograph.

Unreinforced copper specimens tested in this investigation showed a very small reduction in area and gave a brittle stress-rupture failure. The photomicrograph presented in figure 26(a) shows the intercrystalline cracking that had occurred. The brittle nature of this failure is shown by the macrophotograph in figure 26(b). This brittle-type behavior is typical of materials tested at very high temperatures in relation to their melting points.

The incorporation of a small amount of fibers (10 vol. %) changes this brittle-type behavior to a very ductile failure (fig. 27) in which the copper almost forms a point at fracture. The fiber-matrix bond is retained because of the small number of fibers and the large amount of matrix present. Since there are no intercrystalline stress-rupture cracks in the matrix, it serves as an indication that the matrix of the composite did not undergo the large amount of third-stage creep normally found in copper. The majority of strain was probably all nearly instantaneous after the failure of the fibers.

Specimens with greater fiber contents showed a less ductile fracture. A macrophotograph of a typical specimen is presented in figure 28(a). The composite has necked and exhibits about a 20-percent reduction in area at fracture. A photomicrograph typical of this behavior is presented in figure 28(b) and it shows that the fibers have necked and exhibit about the same reduction in area as when tested individually. The fiber-matrix bond has been destroyed at the fracture during the necking of the fibers. Although the individual fibers showed about the same reduction in area as when tested individually (about 80 percent), the composites showed an apparent ductility of about 20 percent. This reduction in area is misleading, however, because of the splitting of the fiber-matrix bond during the necking process. This splitting indicates that reduction-in-area ductility measurements on fiber-reinforced composites must be carefully scrutinized to examine their validity. A macrophotograph of the fracture surface of a composite (fig. 29) shows that the wire extends beyond the fracture surface of the copper matrix to give a needle-like fracture, which is caused by the tearing away of the fiber-matrix bond during necking.

At fiber contents above about 65 percent, the specimens failed in a manner similar to that shown in the macrophotograph of figure 30. These specimens failed at the tangent where the radius meets the test section. The test section end of the specimen had an inward cone, while the shank piece had an outward cone shape. In some cases, there was also a crack at the other end of the test section at the fillet (fig. 31). In general, the highest fiber-content specimens showed this double cracking. An enlarged view of a fillet crack is shown in figure 32.

The fourth type of composite failure was a shear failure, shown in figure 33. This type of failure again occurred with the higher fiber-content specimens. Instead of a fracture initiated at the surface of the test section at the fillet and extending circumfer-

entially around the specimen at the line of tangency, this type of failure initiated at opposite sides of the specimens at each end of the test section and fillet. The specimen then failed along a shear plane, parallel to the tensile axis, through the matrix or fiber-matrix interface. The data for this type of failure were not included in this report since specimens exhibiting this type of failure resulted in very reduced lives.

Application to Practical Composites

The results obtained in this investigation show the promise of fiber-reinforced metallic composites for stress-rupture applications. Although the composite components for this model system study were chosen primarily for mutual insolubility, the composites were very strong.

A comparison of the 100-hour rupture strength for several copper-base materials at 1500° F is presented in figure 34. While the dispersion-strengthened copper (ref. 20) shows a significant strength increase over unalloyed pure copper, the tungsten-fiber-reinforced copper composites showed much greater strengths. In fact, composites reinforced with 50-volume-percent fiber showed a strength increase of a factor of 150 times greater than the strength of unreinforced copper, and the strength advantage increases with greater fiber contents. In view of the stability of tungsten wires at this temperature (ref. 16), it would be expected that the stress-rupture properties of the composite would not drop off until close to the melting temperature of the copper matrix.

A plot of 100-hour rupture strength and 100-hour rupture-strength density at 1500° F for two of the better superalloys (refs. 21 to 23) and for tungsten-fiber-reinforced copper composites is presented in figure 35. In this plot, the properties of the composites are shown as a function of fiber content. This plot also shows that the 100-hour rupture strength of the composites compares favorably with the superalloys at intermediate fiber contents. At higher fiber contents, the properties of the composites are superior to those of the superalloys. In spite of the high density of tungsten wire, this plot shows that the 100-hour rupture-strength to density ratio of the composites compares favorably with that of the superalloys. The plot also shows that the rupture-strength to density ratio of composites is not a linear function of fiber content. Since the strength increase with fiber content is greater than the density increase, the slope is higher and the increase per unit fiber content is greater at lower fiber contents.

The encouraging result obtained in this investigation of a model system shows the potential that might be expected from fiber composites for stress-rupture applications. With the proper combination of fabrication technique and choice of materials, practical composites may be made, particularly for use in the temperature range of 2000° to 2500° F. This temperature range is too high to use available nickel- and cobalt-base

superalloys. Refractory metals and alloys, which have a high strength at these temperatures, lack oxidation resistance.

The criteria for practical composite matrix selection would include strength at the desired application temperature, oxidation resistance, compatibility with the reinforcing fiber, and other specific properties of interest. Unfortunately, many of the potential matrix materials having oxidation resistance are not very compatible with tungsten and other refractory metals. References 9, 10, 14, 15, and 18 showed that materials which are soluble or which react with the fiber may reduce the tensile properties of the fiber and, thus, of the composite. Through the use of alloying additions to reduce the chemical potential for diffusion of the components (refs. 14 and 15) and through the expeditious use of fabrication techniques (ref. 24), the deleterious effects of alloying and reaction can be reduced to allow the fabrication of composites with attractive properties. Through proper selection of components and fabrication techniques, refractory-metal-fiber-reinforced superalloy-matrix composites with superior engineering properties can be developed for use in this temperature range.

CONCLUSIONS

An analysis was made to relate the stress-rupture and creep properties of fiber-reinforced composites to those of the components. Predictions based on this analysis were compared with data obtained for tungsten-fiber-reinforced copper composites. The failure mechanism of these composites was also analyzed. The potential of practical composite systems was indicated by extrapolation of the results obtained for the model composite system investigated. The results obtained were as follows:

1. Equations were formulated that can be used to predict the stress - creep rate relations of composites based on the properties of the components in the condition in which they exist in the composite. When suitable assumptions are used, a simplified version of this equation has the form

$$\sigma_c = \left[\left(\sigma_f\right)_o A_f + \left(\sigma_m\right)_o A_m\right]\dot{\epsilon}^{\psi}$$

The creep behavior of tungsten-fiber-reinforced copper composites was in good agreement with this equation.

2. Equations were also formulated that can be used to predict the stress-rupture life of composites based on the properties of the components. When suitable assumptions are made, an approximation, based on the minimum creep rate of the fiber, can be used having the form

$$\sigma_c = \left[\left(\sigma_f\right)_1 t^{\omega_f} A_f\right] + \left[\sigma_m\Big|_{\dot{\epsilon}=1}\left(\dot{\epsilon}_f\Big|_{t=1} t_f^{\gamma_f}\right)^{\psi_m} A_m\right]$$

Another approximation, based on the rupture times of each component, also can be used:

$$\sigma_c = \left[\left(\sigma_f\right)_1 A_f + \left(\sigma_m\right)_1 A_m\right] t^{\omega_f}$$

The stress-rupture life of tungsten-fiber-reinforced copper composites was in agreement with this relation.

3. The methods of predictions presented allow the extrapolation of a limited amount of composite data to a more general case for an entire composite system. In addition, the methods are useful in determing fiber properties within composites when the fiber properties cannot be determined externally, such as a reacted fiber or directionally solidified composites.

4. Based on the assumptions made, seven stages of creep deformation were postulated. Each stage represents a compromise between the properties of the components in which the stresses were distributed and redistributed between the components. The seven postulated stages were composite initial loading, composite first-stage creep, composite quasi first-stage creep, composite second-stage creep, composite quasi, second-stage creep, composite third-stage creep, and composite fracture. The mode of fracture of tungsten-fiber-reinforced copper composites appeared to be a function of fiber content. Unreinforced copper gave brittle fractures with a great deal of stress-rupture cracking present. Tungsten wires exhibited ductile fracture with pronounced necking. Composites reinforced with fiber contents below 10 volume percent exhibited a very ductile fracture with the formation of a point. The fiber-matrix bond was intact after fracture. Composites reinforced with fiber contents greater than 10 volume percent exhibited a relatively ductile fracture; however, the reduction in area of the composites was considerably less than that of the fibers alone. This reduction was attributed to the destruction of the fiber-matrix bond during necking.

5. The excellent stress-rupture properties of tungsten wires were fully utilized in tungsten-fiber-reinforced copper composites. The excellent potential of fiber-reinforced composites for stress-rupture applications is indicated by comparisons with competing materials. The rupture strength of tungsten-fiber-reinforced copper composites, studied as a model system, were superior to some of the better superalloys in stress-rupture at 1500° F. The stress-rupture-strength to density ratio of the composites also compared

favorably with some superalloys. Extrapolation of the results obtained from this model system to more practical composites at higher temperatures could be expected to result in the development of engineering materials with superior properties.

Lewis Research Center,
National Aeronautics and Space Administration,
Cleveland, Ohio, April 3, 1967,
129-03-09-01-22.

REFERENCES

1. Jech, R. W.; McDanels, D. L.; and Weeton, J. W.: Fiber Reinforced Metallic Composites. Composite Materials and Composite Structures. Proceedings of the Sixth Sagamore Ordnance Materials Research Conference, Racquette Lake, New York, Aug. 18-21, 1959. Rep. No. MET661-601, Syracuse University Research Institute, 1959, pp. 116-143.

2. McDanels, D. L.; Jech, R. W.; and Weeton, J. W.: Metals Reinforced with Fibers. Metal Progress, vol. 78, no. 6, Dec. 1960, pp. 118-121.

3. McDanels, David L.; Jech, Robert W.; and Weeton, John W.: Stress-Strain Behavior of Tungsten-Fiber-Reinforced Copper Composites. NASA TN D-1881, 1963.

4. McDanels, D. L.; Jech, R. W.; and Weeton, J. W.: Analysis of Stress-Strain Behavior of Tungsten-Fiber-Reinforced Copper Composites. AIME Trans., vol. 233, no. 4, Apr. 1965, pp. 636-642.

5. McDanels, David L.: Electrical Resistivity and Conductivity of Tungsten-Fiber-Reinforced Copper Composites. NASA TN D-3590, 1966.

6. Sutton, Willard H.: Development of Composite Structural Materials for Space Vehicle Applications. ARS J., vol. 32, no. 4, Apr. 1962, pp. 593-600.

7. Cratchley, D.; and Baker, A. A.: The Tensile Strength of a Silica Fibre Reinforced Aluminum Alloy. Metallurgia, vol. 69, no. 414, Apr. 1964, pp. 153-159.

8. Kelley, A.; and Tyson, W. R.: Fibre-Strengthened Materials. High-Strength Materials, 2nd International Materials Conference, Berkeley, Calif., V. F. Zackay, ed., John Wiley and Sons, Inc., 1965, pp. 578-602.

9. Petrasek, Donald W.: Elevated-Temperature Tensile Properties of Alloyed Tungsten Fiber Composites. NASA TN D-3073, 1965.

10. Petrasek, Donald W.: Elevated-Temperature Tensile Properties of Tungsten Fiber Composites. AIME Trans., vol. 236, no. 6, June 1966, pp. 887-896.

11. Jech, R. W.; Weber, E. P.; and Schwope, A. D.: Fiber-Reinforced Titanium Alloys. Reactive Metals. Vol. 2. W. R. Clough, ed., Interscience Publishers, 1959, pp. 109-119.

12. Dean, A. V.: The Reinforcement of Nickel-Base Alloys with High Strength Tungsten Wires. Rep. No. NGTE-R. 266, Nation Gas Turbine Establishment, Apr. 1965. (Available from DDC as AD-464771.)

13. Ellison, E. G.; and Harris, B.: The Elevated Temperature Properties of a Nickel Alloy Reinforced with Tungsten Wires. Appl. Materials Res., vol. 5, no. 1, Jan. 1966, pp. 33-40.

14. Petrasek, Donald W.; and Weeton, John W.: Alloying Effects on Tungsten-Fiber-Reinforced Copper-Alloy or High-Temperature-Alloy Matrix Composites. NASA TN D-1568, 1963.

15. Petrasek, Donald W.; and Weeton, John W.: Effects of Alloying on Room-Temperature Tensile Properties of Tungsten-Fiber-Reinforced-Copper-Alloy Composites. AIME Trans., vol. 230, no. 5, Aug. 1964, pp. 977-990.

16. McDanels, David L.; and Signorelli, Robert A.: Stress-Rupture Properties of Tungsten Wire from 1200° to 2500° F. NASA TN D-3467, 1966.

17. Jech, R. W.; Springborn, R. H.; and McDanels, D. L.: Apparatus for Stress-Rupture Testing of Filaments in a Controlled Environment. Rev. Sci. Instr., vol. 35, no. 3, Mar. 1964, pp. 314-315.

18. Signorelli, R. A.; Petrasek, D. W.; and Weeton, J. W.: Interfacial Reactions in Metal-Metal and Ceramic-Metal Fiber Composites. Modern Composite Materials. Richard Krock and Lawrence Broutman, eds., Addison-Wesley Publ. Co., 1967.

19. Jenkins, William D.; and Johnson, Carl R.: Creep of Annealed Nickel, Copper, and Two Nickel-Copper Alloys. J. Research Natl. Bur. Standards, vol. 60, no. 3, Mar. 1958, pp. 173-191.

20. Preston, Oliver; and Grant, Nicholas J.: Dispersion Strengthening of Copper by Internal Oxidation. AIME Trans., vol. 221, no. 1, Feb. 1961, pp. 164-173.

21. Lund, C. H.: The Use of Nickel-Base Alloys in the Rotating Parts of Gas Turbines for Aerospace Applications. Memo No. 145, Defense Metals Information Center, Jan. 1962.

22. Van Echo, John A.; and Simmons, Ward F.: Mechanical and Physical Properties of Three Superalloys - MAR-M200, MAR-M302, and MAR-M322. DMIC Memo 193, Battelle Memorial Inst., May 6, 1964.

23. Campbell, J. E.: Compilation of Tensile Properties of High-Strength Alloys. DMIC Memo 150, Batelle Memorial Inst., Apr. 23, 1962.

24. Arridge, R. G. C.; Baker, A. A.; and Cratchley D.: Metal Coated Fibres and Fibre Reinforced Metals. J. Sci. Instr., vol. 41, no. 5, May, 1964, pp. 259-261.

TABLE I. - STRESS-RUPTURE PROPERTIES OF TUNGSTEN WIRES ANNEALED UNDER CONDITIONS OF INFILTRATION

[1/2 hr in hydrogen at 2200° F; 1/2 hr in vacuum at 2200° F.]

Test temperature, °F	Stress, psi	Rupture time, hr
1200	165 000	46.0
	160 000	65.9
	160 000	142.8
	155 000	295.6
1500	145 000	0.7
	135 000	4.3
	130 000	14.0
	130 000	33.1
	125 000	62.3
	120 000	157.6
	120 000	311.0
	120 000	377.5

TABLE II. - STRESS TO CAUSE RUPTURE IN 1, 10, AND 100 HOURS FOR 5-MIL-DIAMETER TUNGSTEN WIRE

Temperature °F	Treatment	Rupture life, hr			
		1	10	100	1000
		Stress to cause rupture, psi			
1200	As-received[a]	198 900	175 400	154 800	136 500
	As-annealed	182 500	171 000	160 300	150 200
1500	As-received[a]	145 500	130 300	116 600	104 400
	As-annealed	142 300	132 600	123 700	115 300

[a]Data for the as-received tungsten wire was taken from ref. 16.

TABLE III. - STRESS-RUPTURE DATA

FOR ANNEALED COPPER-

COPPER SPECIMENS

Temperature, °F	Stress, psi	Rupture time, hr
1200	1990	1.4
	1710	4.0
	1310	11.0
	1190	7.6
	980	18.9
	890	9.3
	690	152.2
	500	357.6
1500	1180	0.5
	1000	1.2
	920	.7
	680	7.0
	620	9.0
	580	13.7
	480	25.1
	380	94.3

TABLE IV. - STRESS TO CAUSE RUPTURE

IN 1, 10, 100, AND 1000 HOURS

FOR COPPER

Temperature, °F	Rupture life, hr			
	1	10	100	1000
	Stress to cause rupture, psi			
1200	2049	1186	686	397
1500	973	607	379	236

TABLE V. - STRESS-RUPTURE RESULTS OF TUNGSTEN-FIBER-REINFORCED COPPER COMPOSITES TESTED AT 1200° F IN PURIFIED HELIUM ATMOSPHERE

Composite stress, psi	Rupture life, hr	Fiber, vol. %
130 000	BOL[a]	62.0
	0.1	67.5
	1.5	63.4
	24.8	71.9
	153.7	75.8
	220.4	75.6
120 000	BOL[a]	49.4
	BOL[a]	50.8
	3.1	63.9
	17.2	63.8
	23.2	67.1
	106.9	71.0
100 000	BOL[a]	18.0
	BOL[a]	44.8
	1.7	49.6
	10.3	55.1
	205.3	59.5
	789 +	64.7
90 000	BOL[a]	30.6
	18.7	44.8
	22.3	49.5
	194.7	61.4
	552.3	60.6
	738.8	59.1
70 000	BOL[a]	29.4
	BOL[a]	30.9
	BOL[a]	31.0
	67.3	37.0
	133.4	39.8
	139.0	39.0
	377.1	51.9
	916.9	48.8
50 000	BOL[a]	12.8
	3.7	25.8
	17.7	28.0
	31.3	29.1
	336.4	33.6
	365.0	31.3
	1434 +	42.6
30 000	127.4	16.6
20 000	BOL[a]	4.7
20 000	BOL[a]	6.2
10 000	38.9	5.8

[a]Broke on loading.

TABLE VI. - STRESS-RUPTURE RESULTS OF TUNGSTEN-FIBER-REINFORCED COPPER COMPOSITES TESTED AT 1500° F IN PURIFIED HELIUM ATMOSPHERE

Composite stress, psi	Rupture life, hr	Fiber, vol. %
100 000	BOL[a]	51.1
	BOL[a]	52.9
	0.3	71.8
	2.9	72.7
	3.8	70.4
	5.2	72.9
	11.9	72.7
95 000	0.5	71.3
	2.7	66.5
	56.8	70.8
	173.2	75.3
90 000	BOL[a]	47.6
	0.1	57.2
	2.1	73.0
	18.5	77.7
	20.3	65.0
	116.3	70.8
80 000	BOL[a]	44.4
	BOL[a]	45.5
	BOL[a]	47.9
	0.2	59.2
	.4	53.2
	2.9	60.2
	16.5	63.2
	23.3	69.9
	25.7	70.8
	32.2	65.4
	90.1	67.7
75 000	0.2	46.0
	.2	49.0
	1.4	52.9
	4.5	50.6
	5.9	58.1
	8.1	51.6
	20.5	58.4
	69.2	55.2
	113.5	63.8
	190.1	72.8
70 000	1.7	48.2
	41.5	60.0
	59.3	54.0
	72.4	53.6
65 000	5.7	44.4
65 000	12.3	44.9
65 000	589.6	56.2
60 000	BOL[a]	23.8
	BOL[a]	34.4
	0.2	42.9
	.3	39.8
	5.3	39.2
	38.6	44.5
	166.5	50.1
	353.3	60.1
50 000	BOL[a]	32.4
	0.3	30.2
	2.4	38.2
	3.6	36.3
	1140.2	43.8

[a]Broke on loading.

TABLE VII. - CREEP RATES

OF COPPER

Temperature, °F	Stress, psi	Creep rate, percent/hr
1200	1710	8.8×10^{-1}
	1310	2.5
	1190	2.7
	980	5.0×10^{-2}
	690	7.3×10^{-3}
	500	7.0×10^{-3}
1500	680	9.4×10^{-1}
	620	4.0
	580	3.0
	480	6.2×10^{-2}
	380	4.8
	390	3.1
	310	1.4
	310	2.5

TABLE VIII. - STRESSES FOR GIVEN

CREEP RATES OF COPPER

Temperature, °F	Creep rate, percent/hr			
	10^{-1}	10^{-2}	10^{-3}	10^{-4}
	Stress, psi			
1200	1052	641	390	238
1500	461	292	185	117

TABLE IX. - CREEP RATES OF COMPOSITES TESTED AT 1200° AND 1500° F

Composite stress, psi	Fiber, vol. %	Rupture time, hr	Creep rate, percent/hr
130 000	75.8	153.7	6.20×10^{-3}
130 000	75.6	220.4	9.50
130 000	68.7	-----	9.75
120 000	71.0	106.9	1.00×10^{-2}
120 000	72.1	-----	3.43
100 000	59.5	205.3	7.20×10^{-3}
	64.1	-----	1.04
	72.1	-----	2.65
	69.9	-----	2.62
	59.3	-----	4.50
	56.7	-----	1.05×10^{-2}
90 000	61.4	194.7	5.60×10^{-3}
	60.1	552.3	3.70
	59.1	738.8	1.67
	69.9	-----	1.58
	59.3	-----	3.00
	63.1	-----	2.70
80 000	63.1	-----	1.90×10^{-3}
70 000	37.0	67.3	2.26×10^{-2}
	39.8	133.4	4.10×10^{-3}
	39.0	139.0	1.02×10^{-2}
	51.9	377.1	2.65×10^{-3}
	71.3	-----	2.20×10^{-4}
	56.6	-----	6.90×10^{-4}
	48.8	-----	2.37×10^{-3}
50 000	33.6	336.4	6.49×10^{-3}
	31.3	365.0	2.41
	42.6	-----	4.50×10^{-4}
	29.1	-----	1.03×10^{-2}
	30.6	-----	3.22
40 000	30.6	-----	3.30×10^{-3}
40 000	26.6	-----	2.87
30 000	16.6	127.4	7.00×10^{-3}
30 000	21.2	-----	2.17
25 000	21.2	-----	9.00×10^{-4}
20 000	26.6	-----	2.87×10^{-4}
20 000	21.2	-----	3.30
15 000	7.7	-----	3.27×10^{-2}
15 000	9.9	-----	3.29×10^{-3}
10 000	5.8	38.9	3.04×10^{-2}
10 000	7.7	-----	1.79×10^{-3}
10 000	9.9	-----	6.60×10^{-4}

Composite stress, psi	Fiber, vol. %	Rupture time, hr	Creep rate, percent/hr
95 000	75.3	173.2	3.16×10^{-2}
95 000	70.8	56.8	6.10
90 000	70.8	116.3	2.76×10^{-2}
80 000	67.7	90.1	3.16×10^{-2}
80 000	73.6	----	1.38
75 000	55.2	69.2	4.42×10^{-2}
75 000	72.8	190.1	1.86
75 000	73.6	-----	5.70×10^{-3}
70 000	53.6	72.4	2.32×10^{-2}
70 000	47.0	----	5.70
70 000	73.6	----	4.63×10^{-3}
65 000	56.2	589.6	1.77×10^{-2}
65 000	50.9	-----	3.94
65 000	73.6	-----	4.28×10^{-3}
60 000	44.5	38.6	5.25×10^{-2}
	50.1	166.5	3.43
	60.1	353.3	1.46
	50.9	-----	1.32
	73.6	-----	3.49×10^{-3}
50 000	43.8	1140.2	1.00×10^{-2}
	73.6	------	8.50×10^{-4}
	50.9	------	6.52×10^{-3}
	34.4	------	5.14×10^{-2}
	59.3	------	1.90×10^{-3}
40 000	36.0	55.4	2.86×10^{-2}
	28.1	92.9	3.60
	34.2	-----	1.59
	50.9	-----	2.90×10^{-3}
	34.4	-----	2.25×10^{-2}
	59.3	-----	2.05×10^{-4}
	47.5	-----	6.27×10^{-3}
	30.8	-----	2.80×10^{-2}
	35.1	-----	1.75
	36.2	-----	1.83
30 000	25.8	196.8	2.00×10^{-2}
	24.4	310.0	3.70
	34.4	-----	4.67×10^{-3}
	30.8	-----	5.60
	35.1	-----	3.10
20 000	17.0	-----	1.08×10^{-2}
10 000	17.0	-----	4.50×10^{-4}
10 000	10.1	-----	5.29×10^{-3}
10 000	11.2	-----	4.00
5 000	4.7	98.6	7.60×10^{-3}
5 000	4.1	129.1	1.18×10^{-2}
5 000	10.4	-----	1.57×10^{-4}

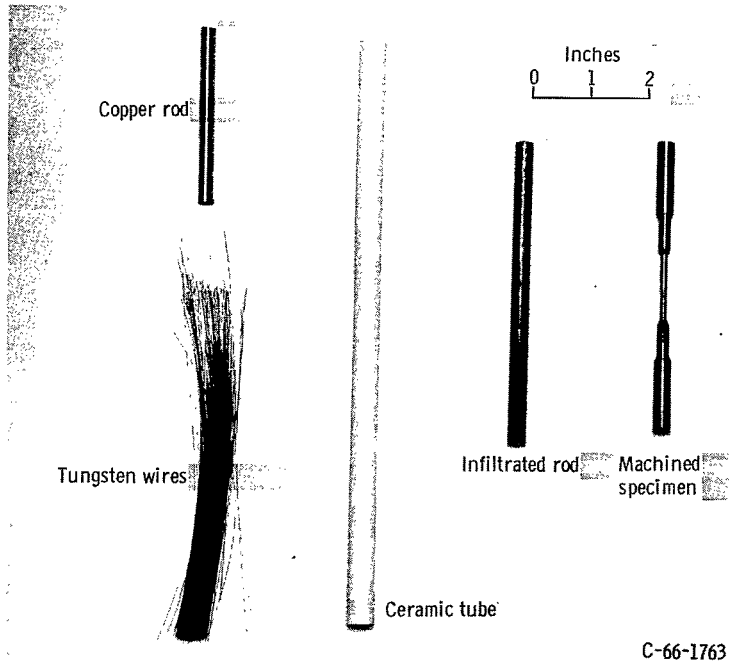

Figure 1. - Speciman preparation of tungsten-fiber-reinforced copper composites.

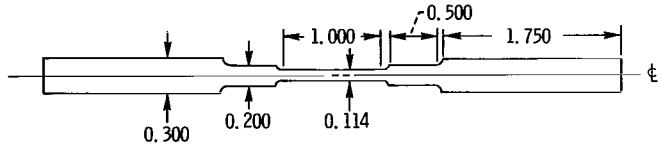

Figure 2. - Specimen used to test tungsten-fiber-reinforced copper composites (all dimensions given in inches).

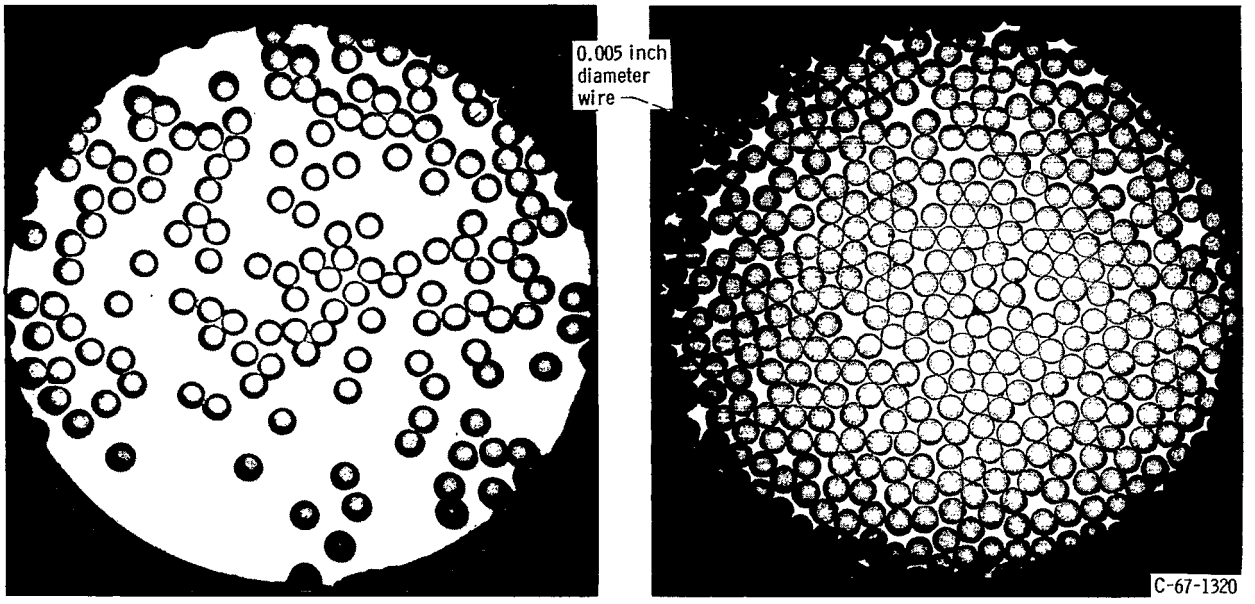

(a) 28.1-Volume-percent tungsten fibers.

(b) 70.8-Volume-percent tungsten fibers.

Figure 3. - Transverse section of tungsten-fiber-reinforced copper composite specimens. Murakami's etchant. X25.

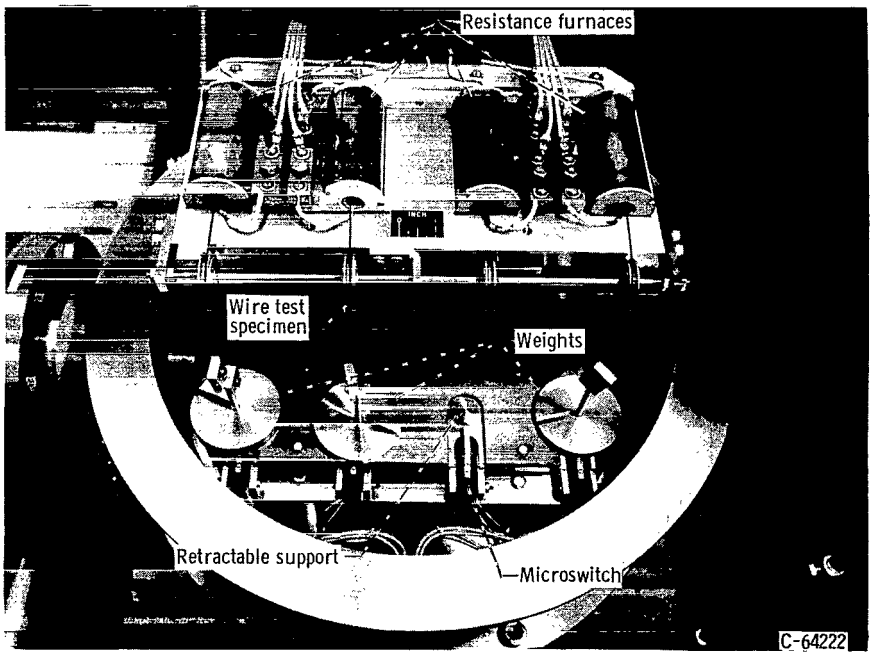

Figure 4. - Filament stress-rupture apparatus showing layout of furnaces, loading train, and microswitches located within environmental chamber.

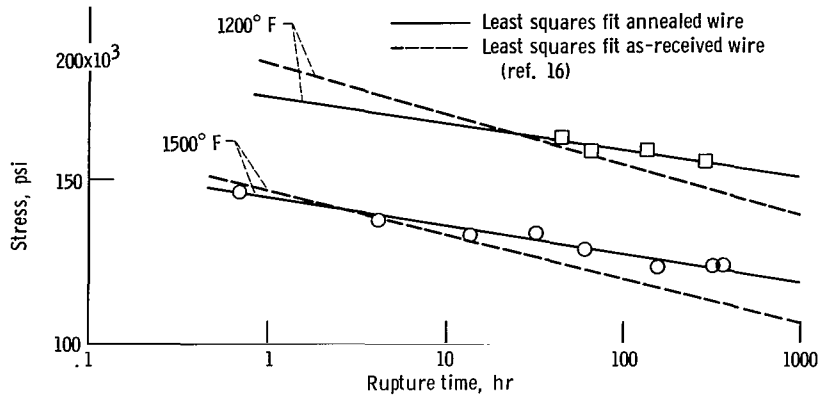

Figure 5. - Rupture time as function of stress for tungsten wire. Wire condition, annealed 1/2 hour in hydrogen at 2200° F; 1/2 hour in vacuum at 2200° F.

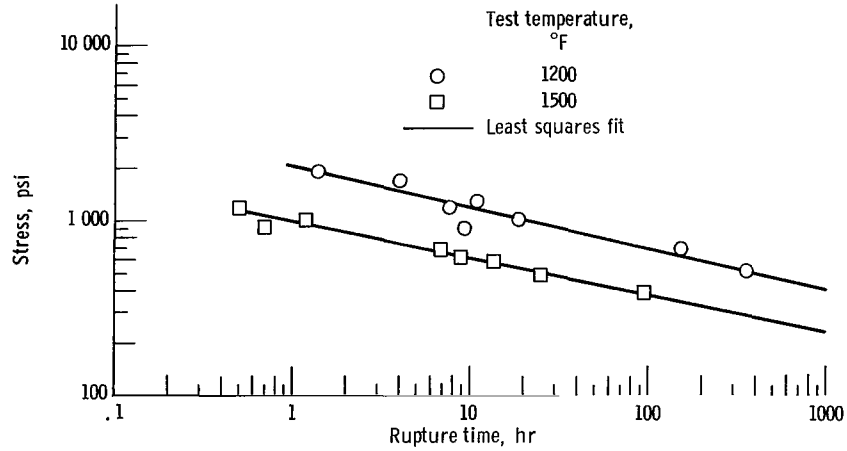

Figure 6. - Stress-rupture properties of copper.

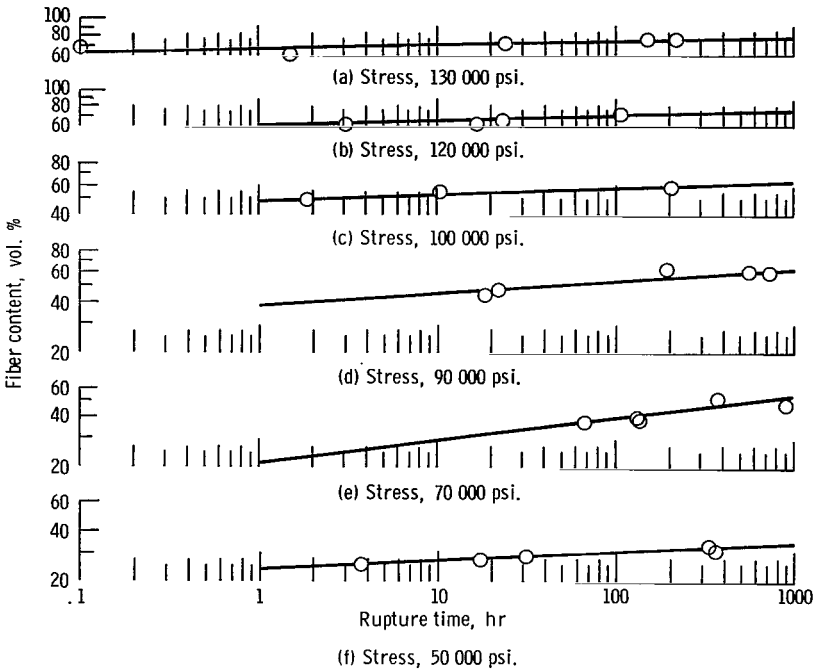

Figure 7. - Rupture time as function of fiber content of composites for various stresses at 1200° F.

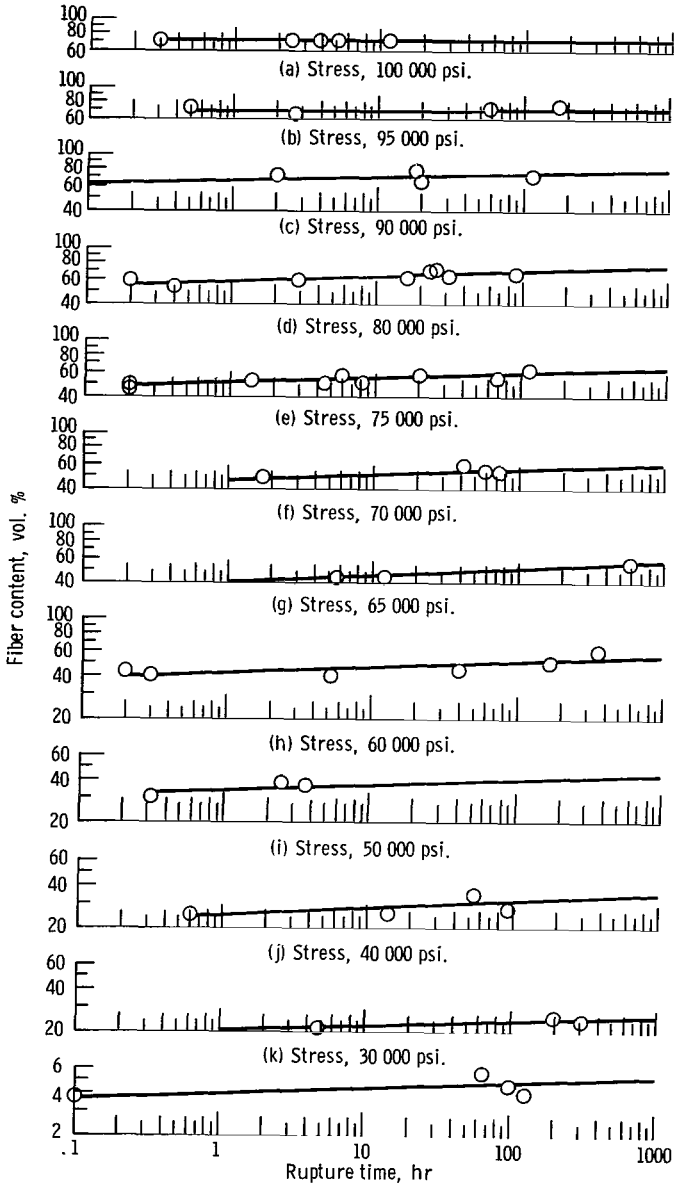

Figure 8. - Rupture time as function of fiber content of composites for various stresses at 1500° F.

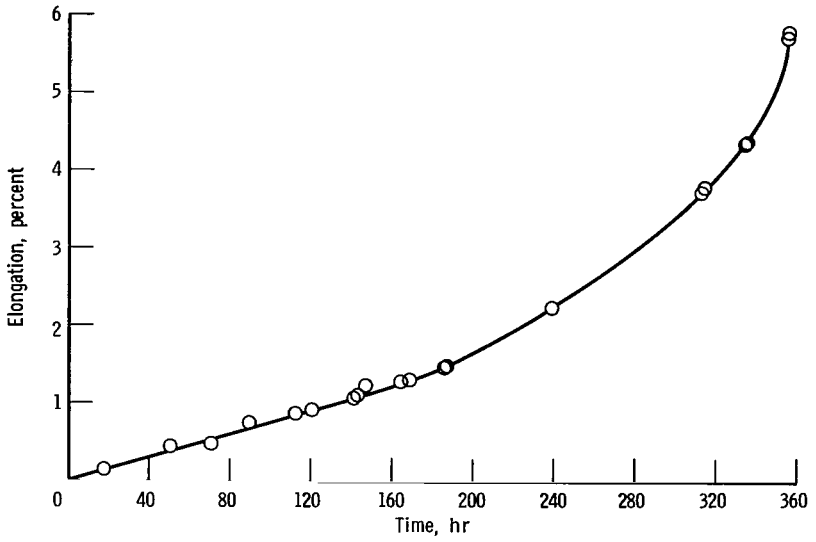

Figure 9. - Typical creep curve of copper specimen tested at 1200° F.

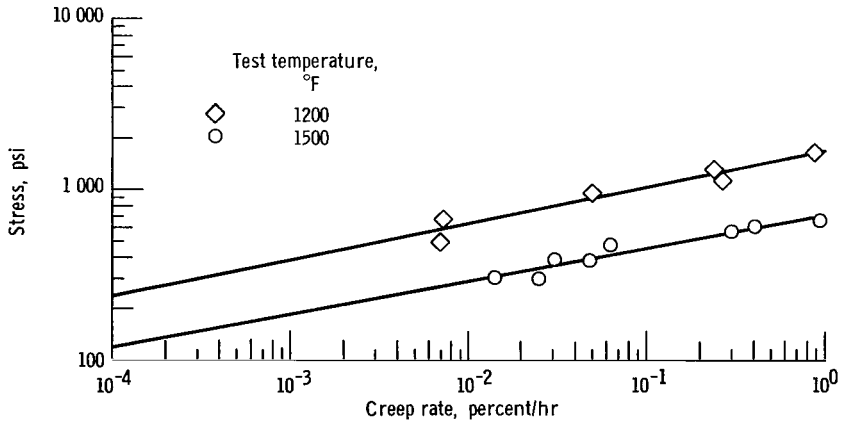

Figure 10. - Creep rate of copper for various stresses.

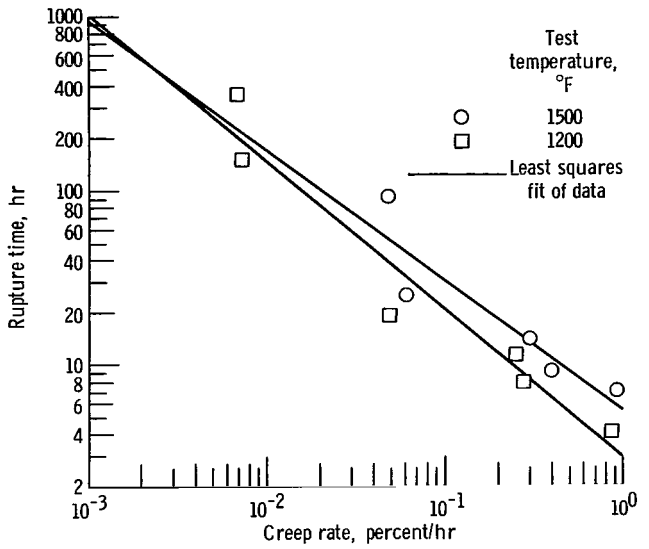

Figure 11. - Rupture time as function of creep rate for copper.

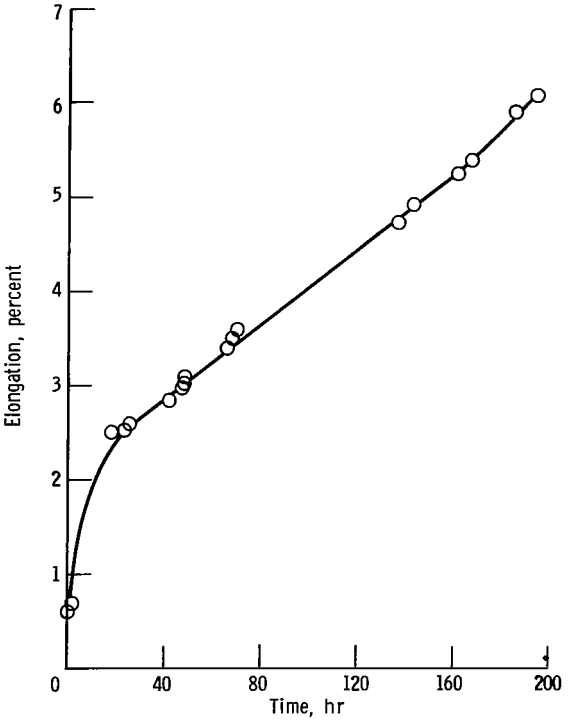

Figure 12. - Typical creep curve of composite specimen tested at 1500° F.

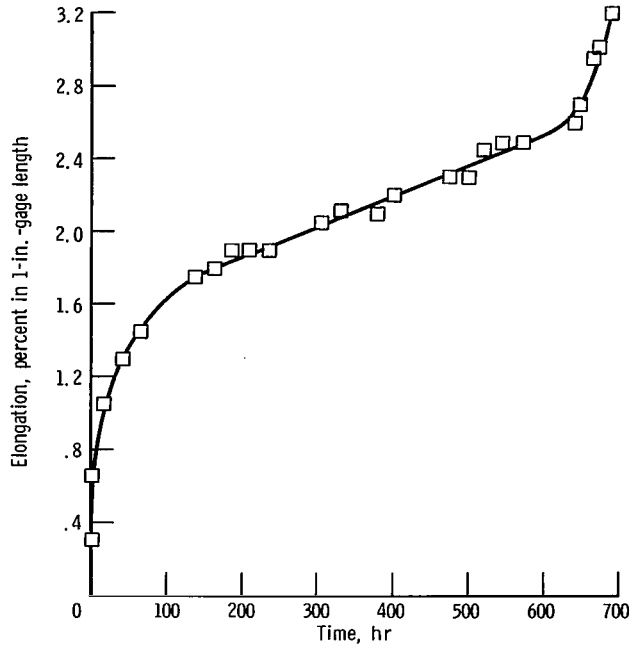

Figure 13. - Typical creep curve of composite specimen tested at 1200° F.

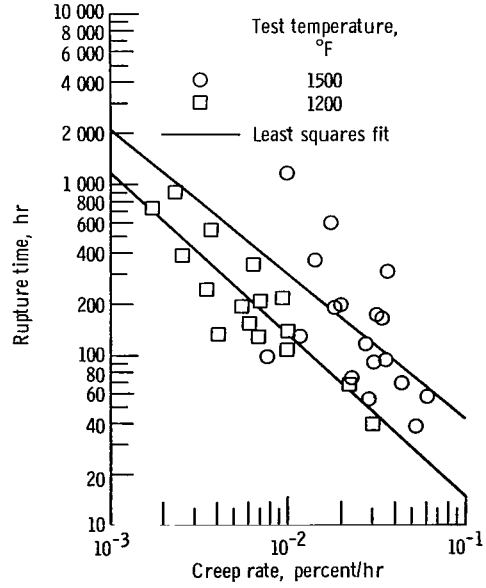

Figure 14. - Rupture time as function of creep rate for composites.

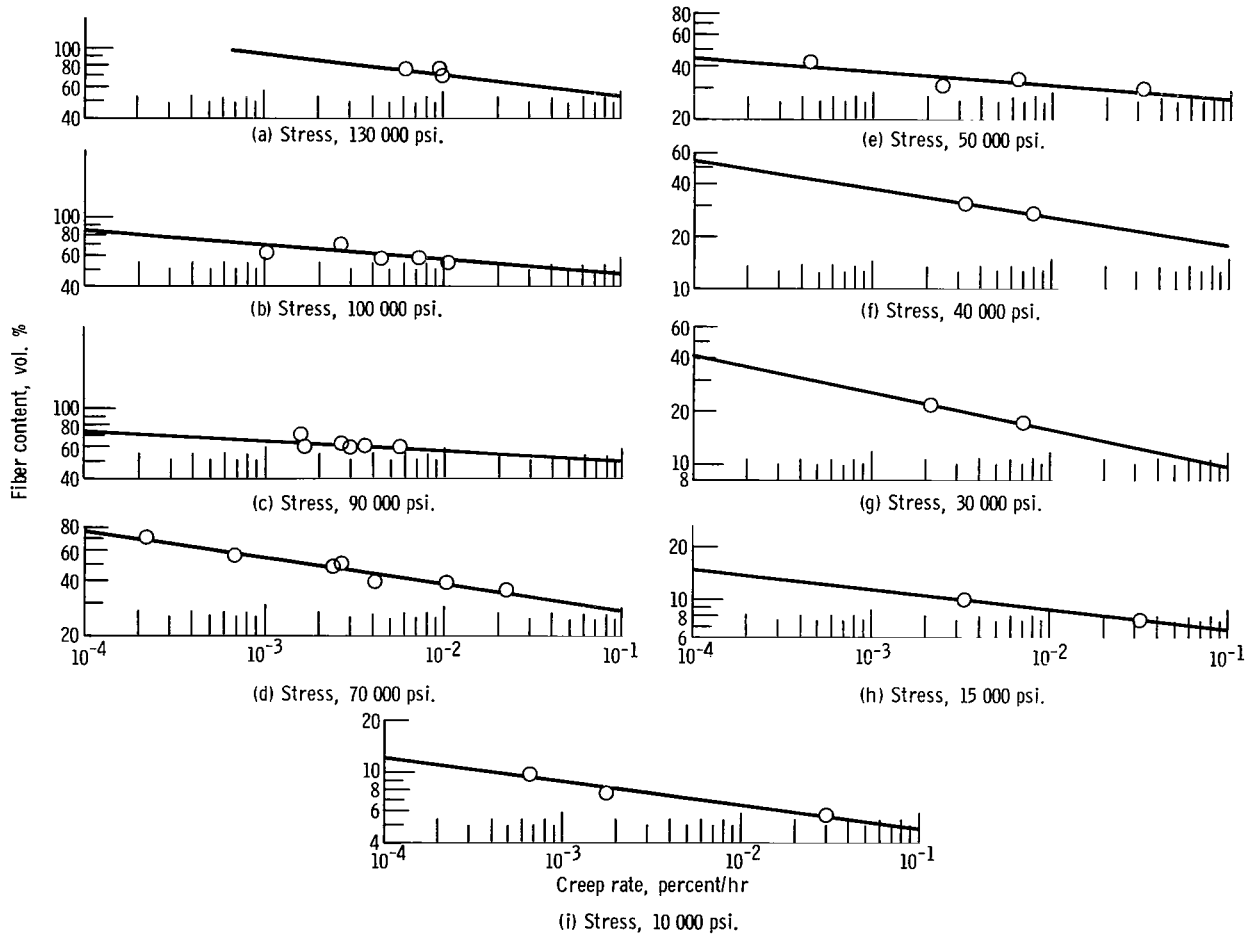

Figure 15. - Fiber content as function of creep rate at various stresses for tungsten-fiber-reinforced copper composites tested at 1200° F.

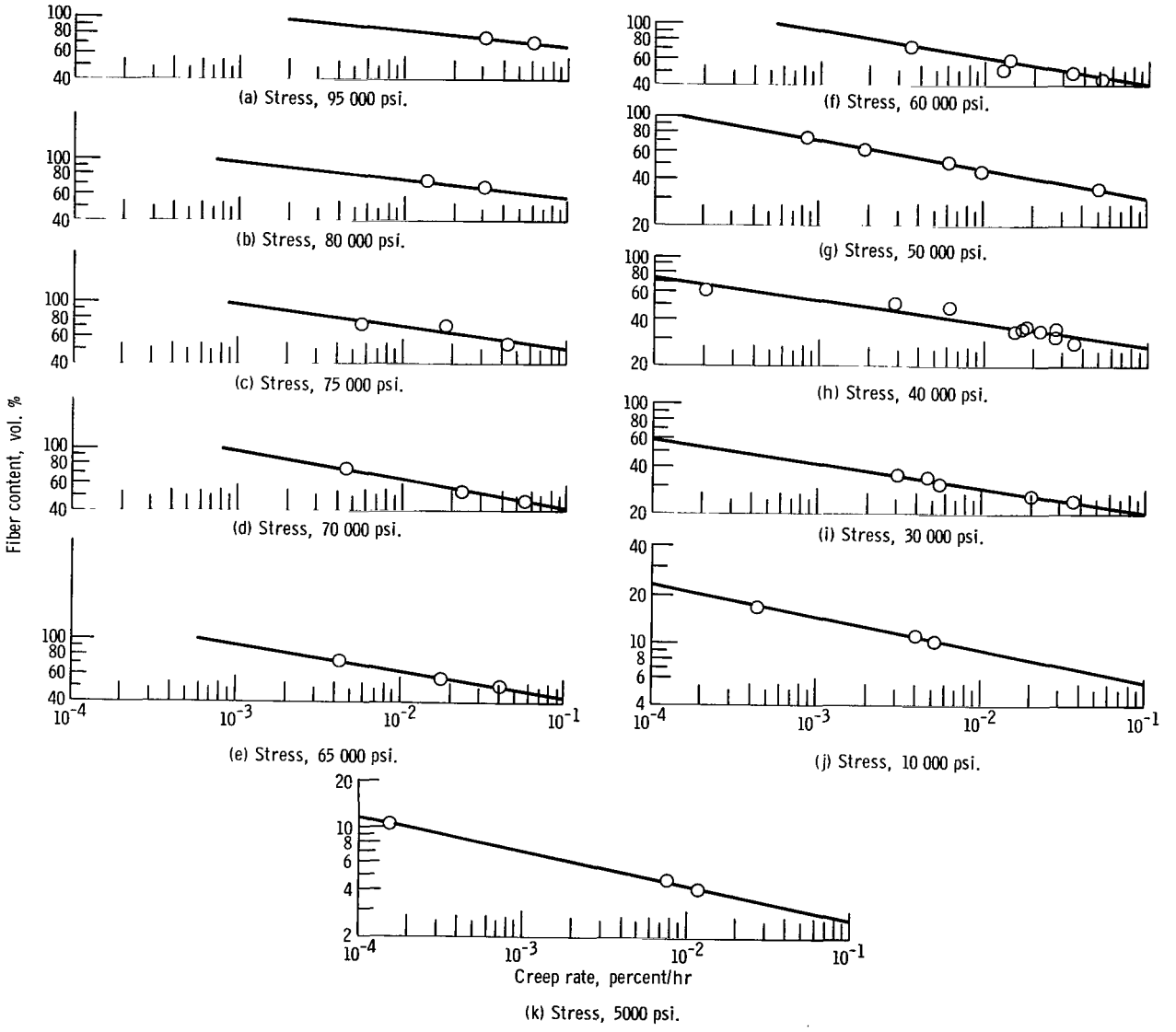

Figure 16. - Fiber content as function of creep rate at various stresses for tungsten-fiber-reinforced copper composites tested at 1500° F.

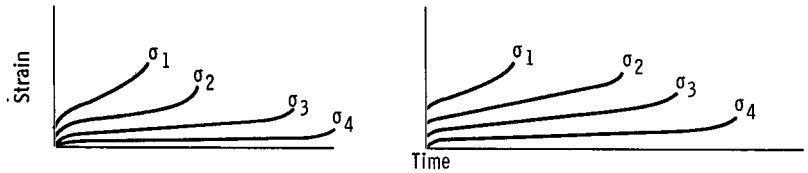

(a-1) Fiber. (a-2) Matrix.

(a) Creep curves of components.

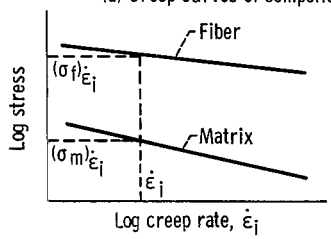

(b) Log stress - log creep rate plots.

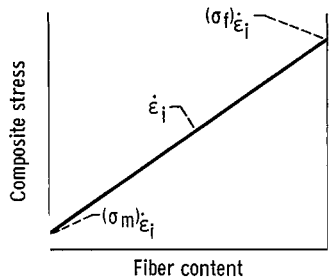

(c) Composite stress - fiber content plot for a given creep rate.

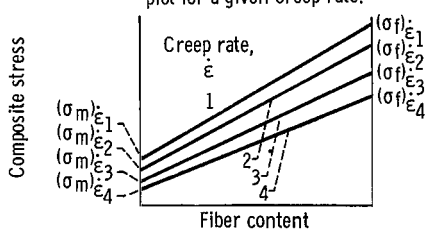

(d) Composite stress - fiber content plot for several creep rates.

Figure 17. - Schematic representation for predicting stresses on composite and components for creep rate calculations.

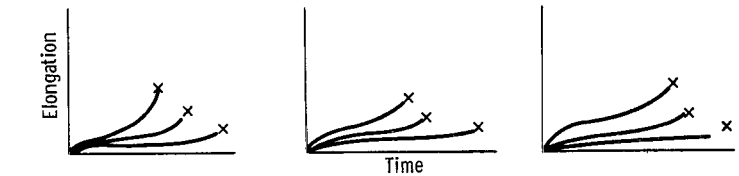

(a-1) Fiber. (a-2) Matrix. (a-3) Composite.

(a) Creep curves.

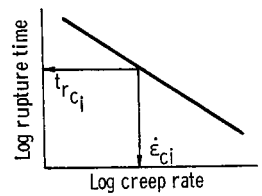

(b) Rupture time - creep rate curve for fiber.

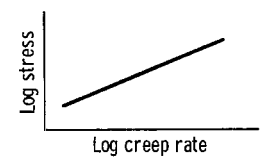

(c) Stress - creep rate curve for matrix.

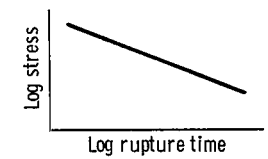

(d) Stress - rupture time curve for fiber.

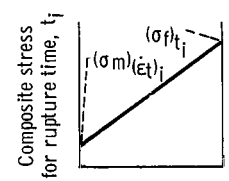

(e) Stress - composition curve for t_i composite rupture time.

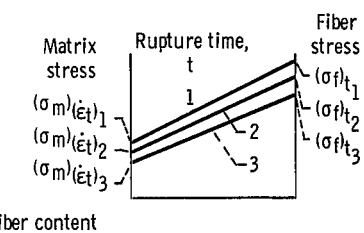

(f) Stress - composition curve for several rupture times.

Figure 18. - Schematic of steps in prediction of rupture time.

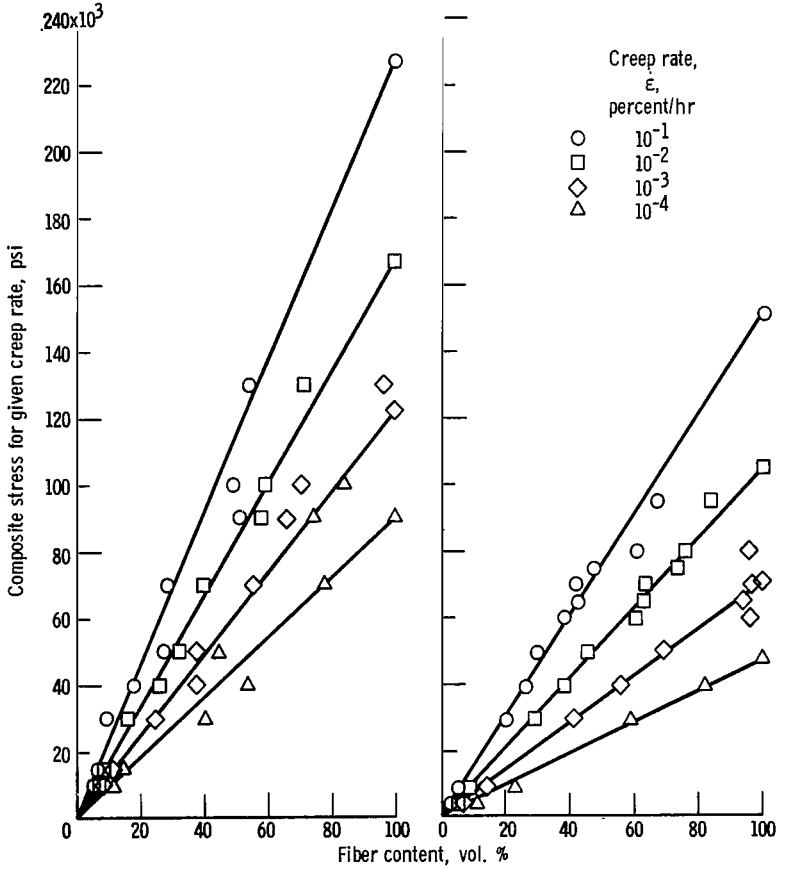

(a) Test temperature, 1200° F. (b) Test temperature, 1500° F.

Figure 19. - Stress for given creep rate as function of fiber content for tungsten-fiber-reinforced composites.

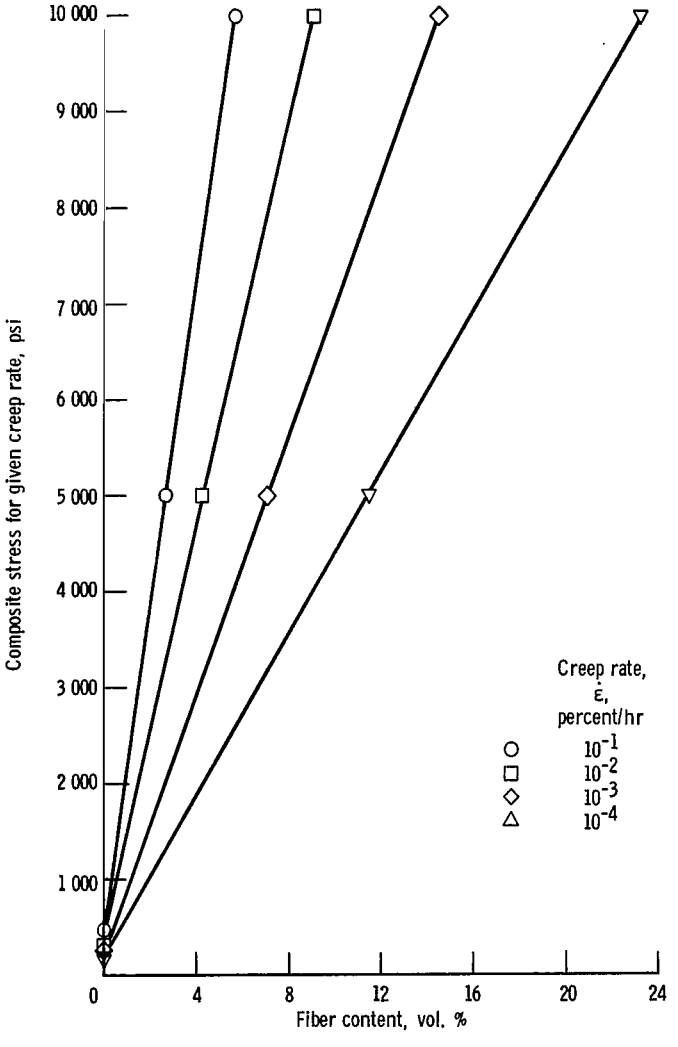

Figure 20. - Enlargement of low-fiber-content region of curve of stress for given creep rate - fiber content.

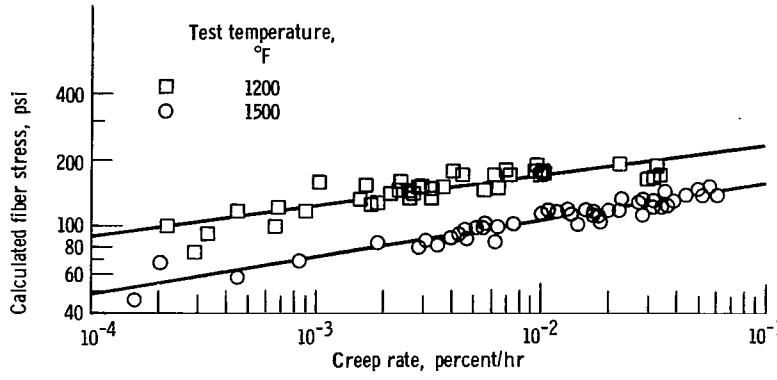

Figure 21. - Log-calculated fiber stress as function of log creep rate for tungsten-fiber-reinforced copper composites.

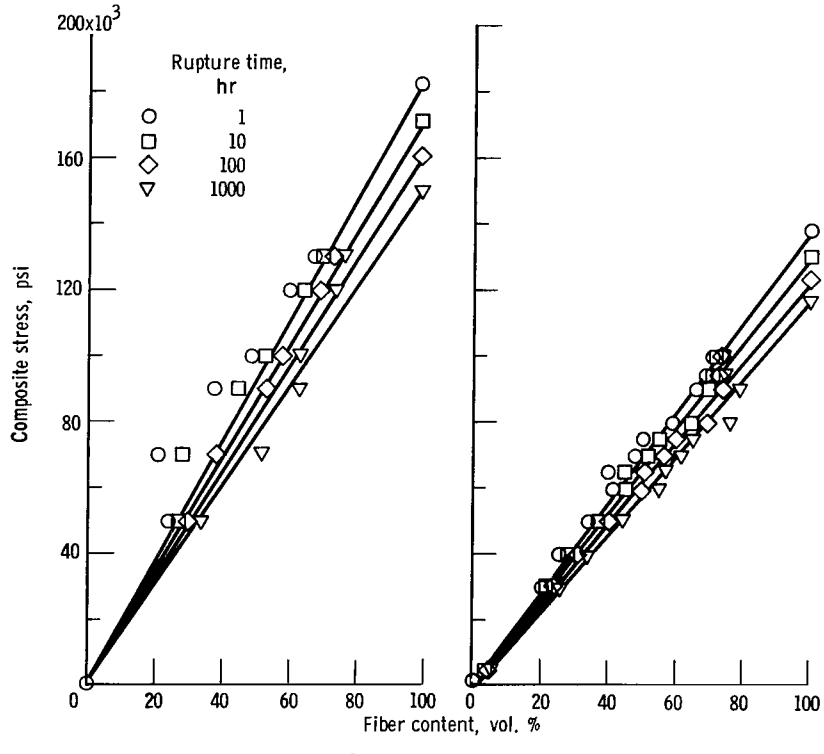

(a) Test temperature, 1200° F. (b) Test temperature, 1500° F.

Figure 22. - Stress to cause rupture in 1, 10, 100, and 1000 hours for tungsten-fiber-reinforced copper composites.

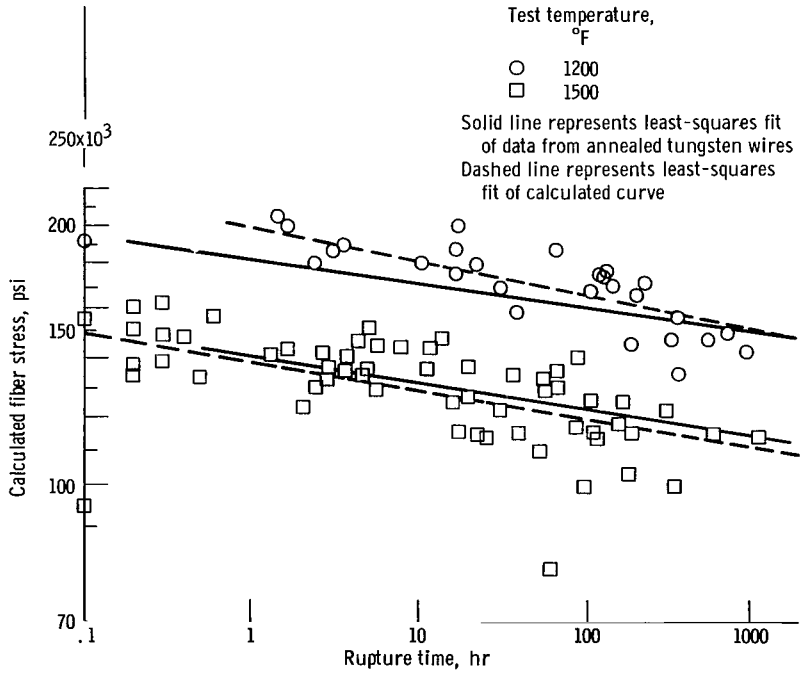

Figure 23. - Log-calculated fiber stress as function of log rupture time for composites.

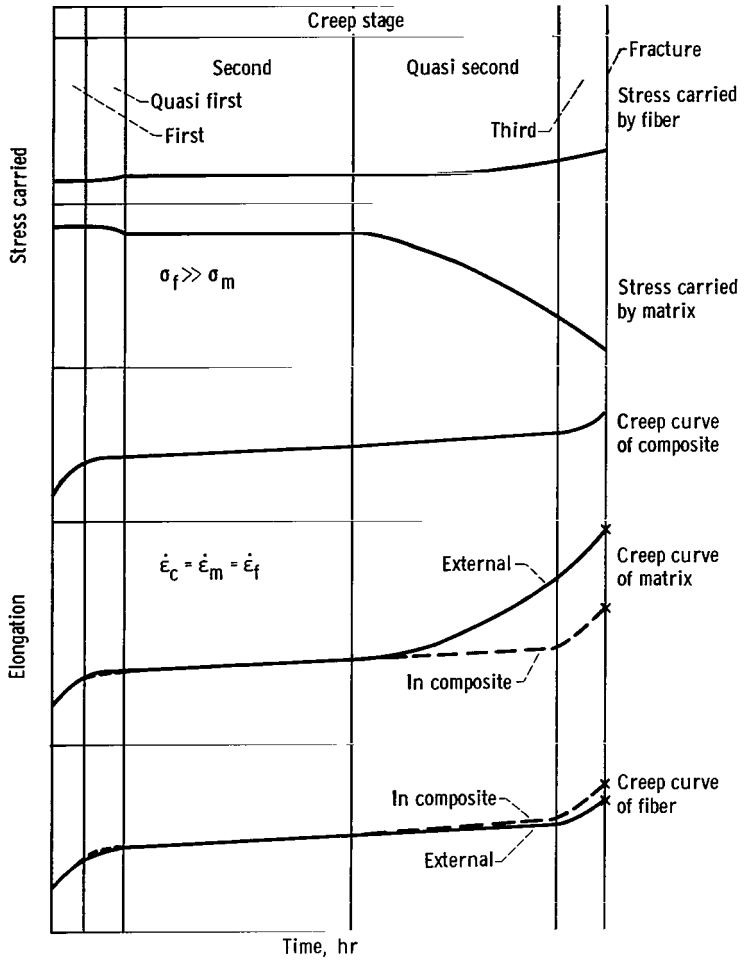

Figure 24. - Schematic of creep curves and stress curves for fiber-reinforced composites. Stress for each component was selected to yield same creep rate and rupture time.

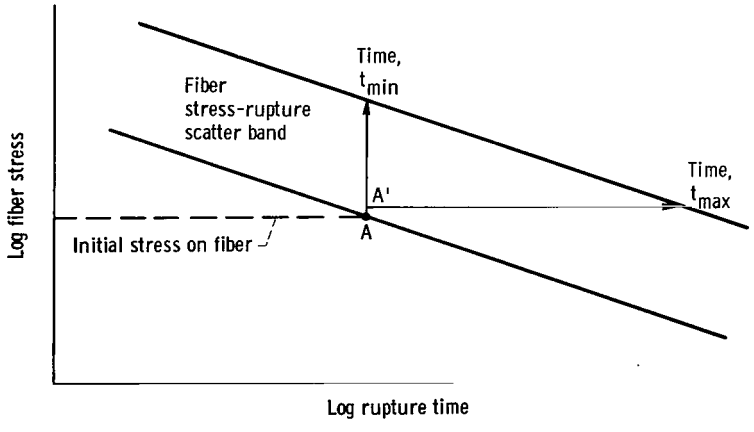

Figure 25. - Schematic diagram of rupture behavior.

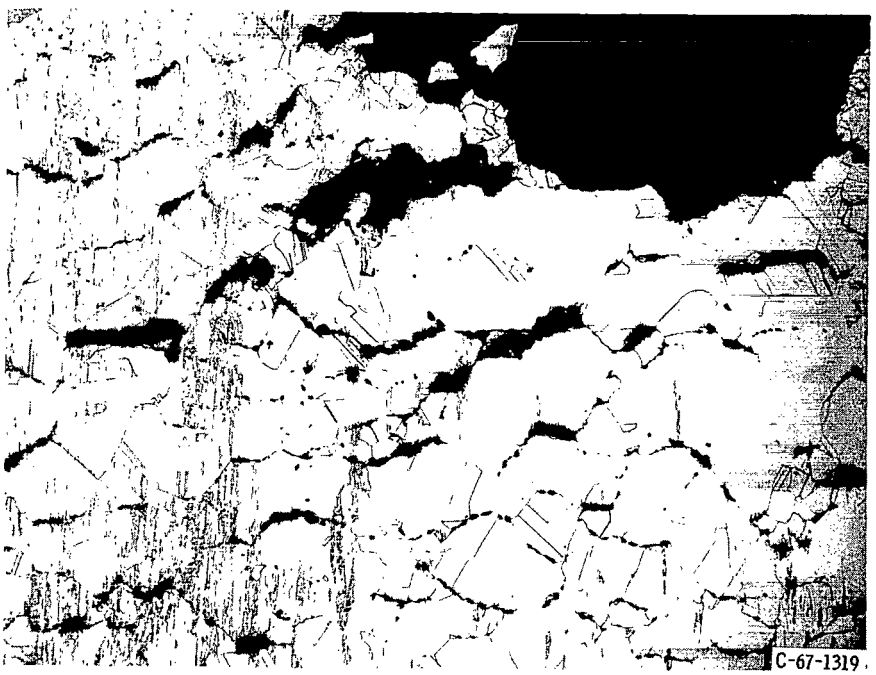

(a) Intercrystalline cracking.

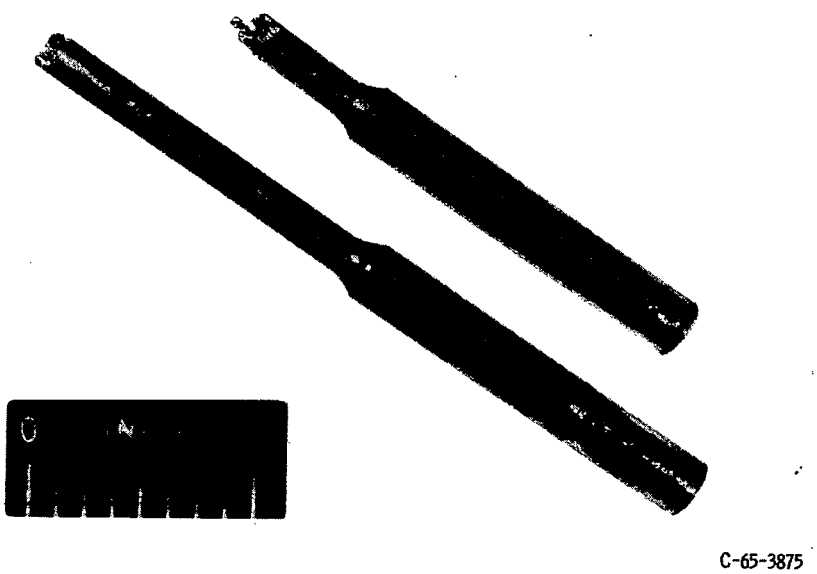

(b) Brittle nature of failure.

Figure 26. - Brittle stress-rupture failure in unreinforced copper specimens.

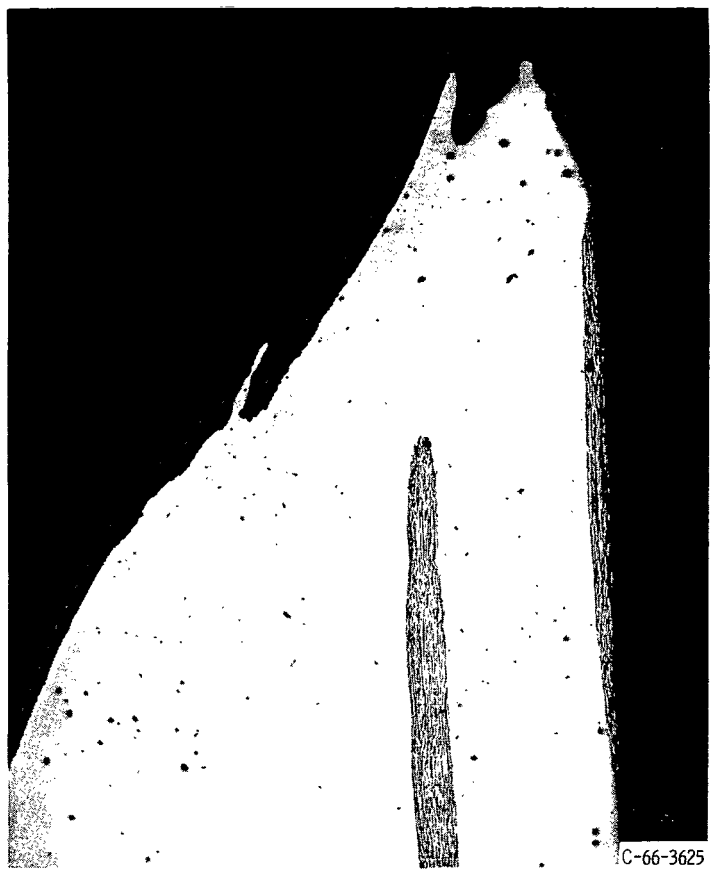

(a) Microphotograph.

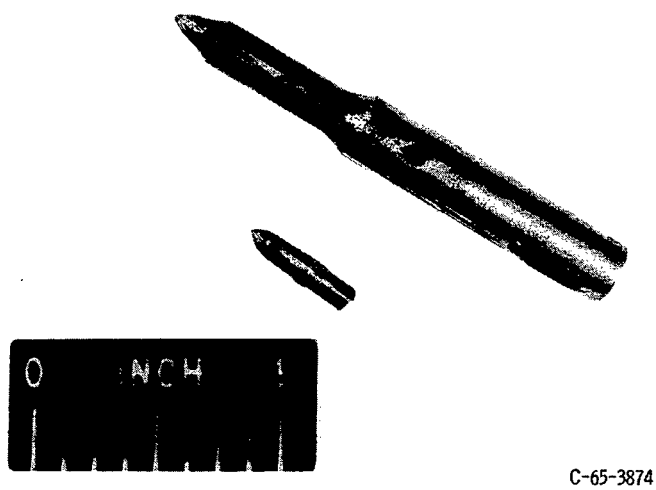

(b) Macrophotograph.

Figure 27. - Ductile failure of composite reinforced with 10-volume-percent fibers.

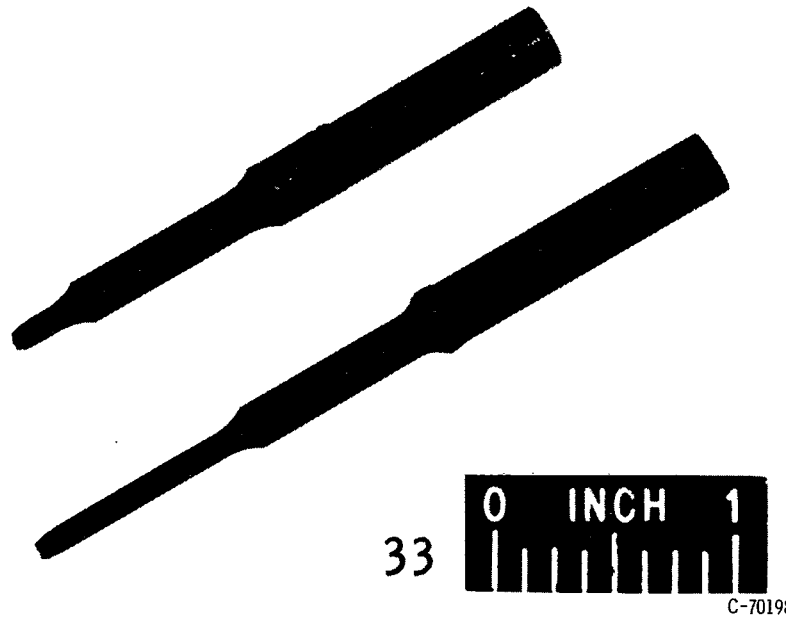

(a) Fracture edge of specimen.

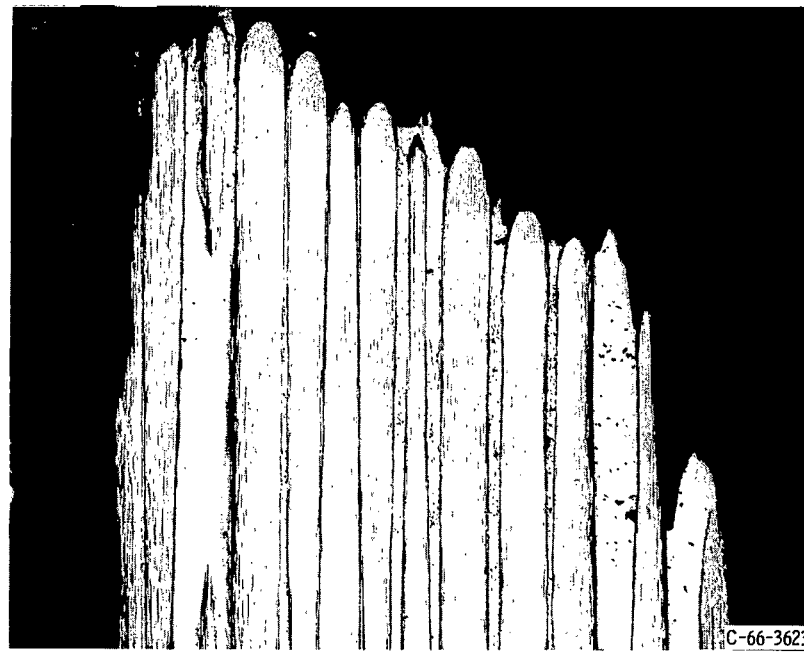

(b) Necking of fibers in typical specimen.

Figure 28. - Fracture in composite with greater fiber contents.

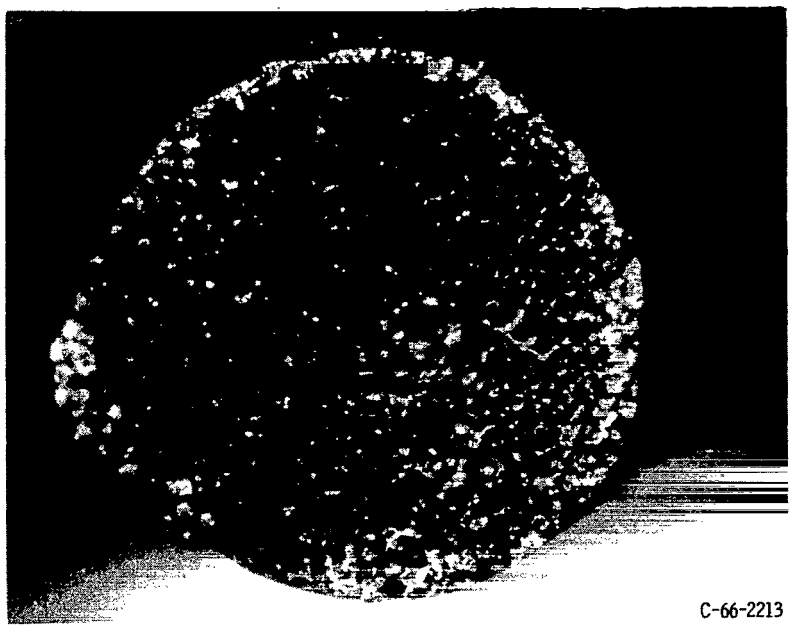

C-66-2213

Figure 29. - Macrophotograph of fracture of composite. X30.

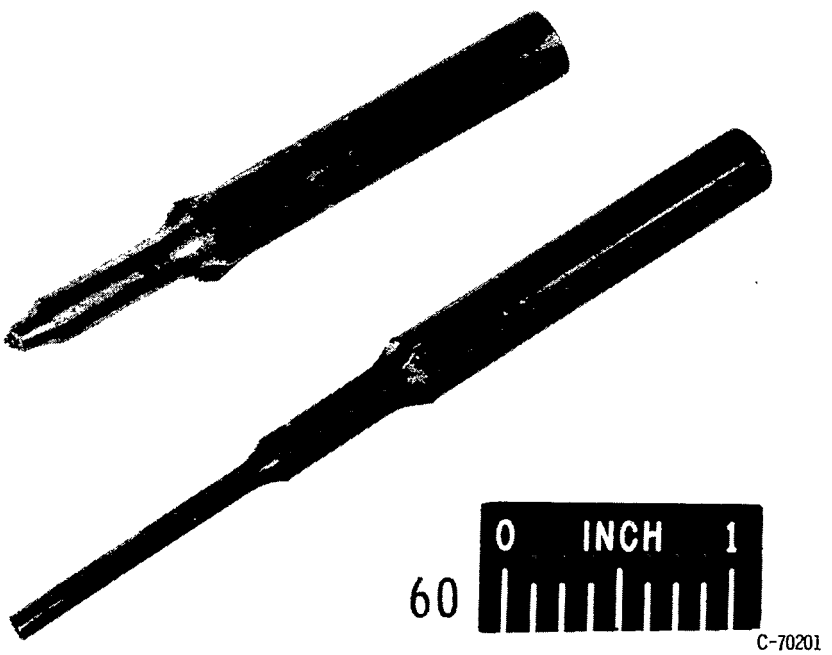

C-70201

Figure 30. - Specimens showing fillet cracking on one end.

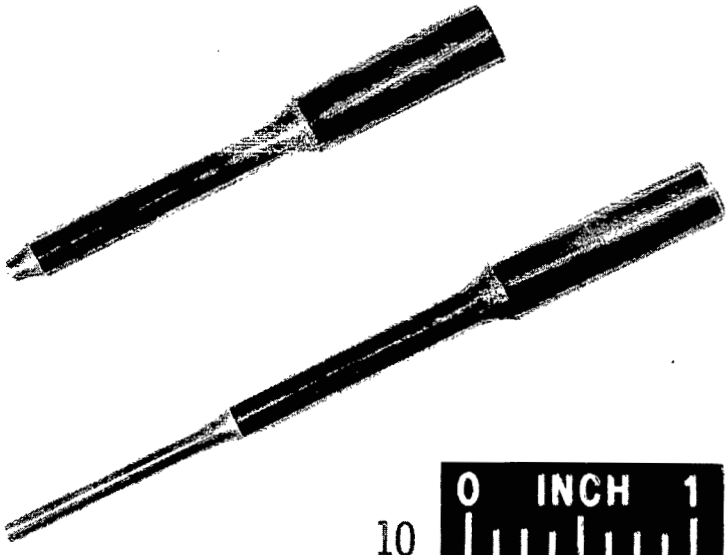

C-70207

Figure 31. - Specimens showing fillet cracks at both ends.

C-66-2211

Figure 32. - Fillet crack.

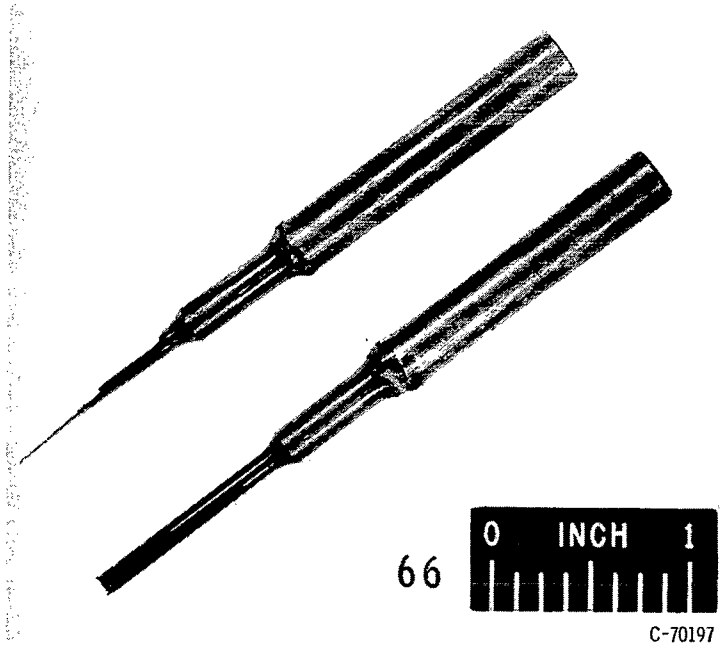

Figure 33. - Specimen showing shear failures.

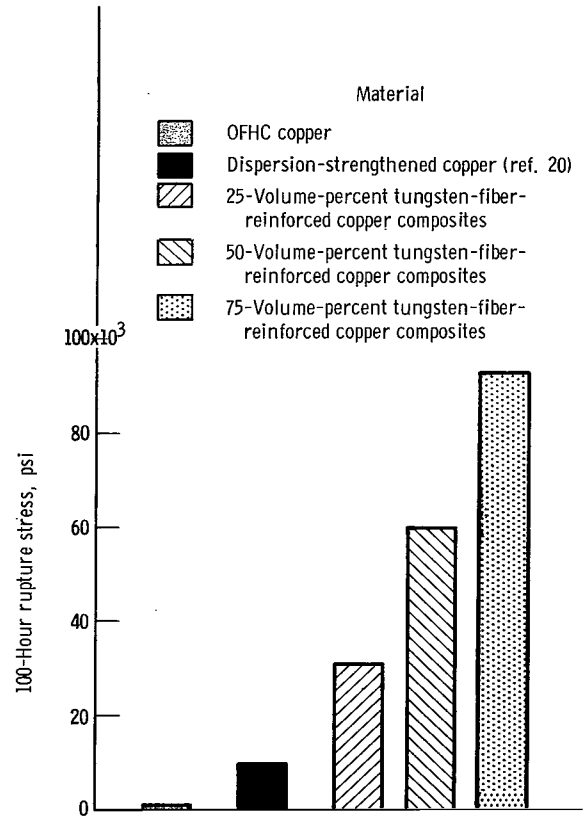

Figure 34. - Comparison of 100-hour rupture strengths of several copper-base materials at 1500° F.

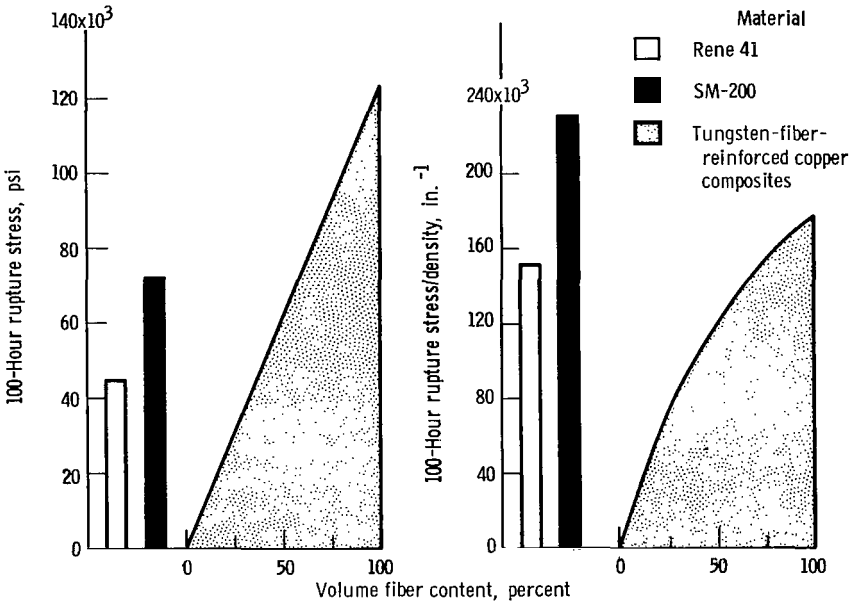

(a) 100-Hour rupture stress. (b) 100-Hour-rupture-stress density.

Figure 35. - Comparison of 100-hour rupture stress and 100-hour-rupture-stress density of tungsten-fiber-reinforced copper composites and superalloys at 1500° F.

"The aeronautical and space activities of the United States shall be conducted so as to contribute . . . to the expansion of human knowledge of phenomena in the atmosphere and space. The Administration shall provide for the widest practicable and appropriate dissemination of information concerning its activities and the results thereof."

—NATIONAL AERONAUTICS AND SPACE ACT OF 1958

NASA SCIENTIFIC AND TECHNICAL PUBLICATIONS

TECHNICAL REPORTS: Scientific and technical information considered important, complete, and a lasting contribution to existing knowledge.

TECHNICAL NOTES: Information less broad in scope but nevertheless of importance as a contribution to existing knowledge.

TECHNICAL MEMORANDUMS: Information receiving limited distribution because of preliminary data, security classification, or other reasons.

CONTRACTOR REPORTS: Scientific and technical information generated under a NASA contract or grant and considered an important contribution to existing knowledge.

TECHNICAL TRANSLATIONS: Information published in a foreign language considered to merit NASA distribution in English.

SPECIAL PUBLICATIONS: Information derived from or of value to NASA activities. Publications include conference proceedings, monographs, data compilations, handbooks, sourcebooks, and special bibliographies.

TECHNOLOGY UTILIZATION PUBLICATIONS: Information on technology used by NASA that may be of particular interest in commercial and other non-aerospace applications. Publications include Tech Briefs, Technology Utilization Reports and Notes, and Technology Surveys.

Details on the availability of these publications may be obtained from:

SCIENTIFIC AND TECHNICAL INFORMATION DIVISION

NATIONAL AERONAUTICS AND SPACE ADMINISTRATION

Washington, D.C. 20546